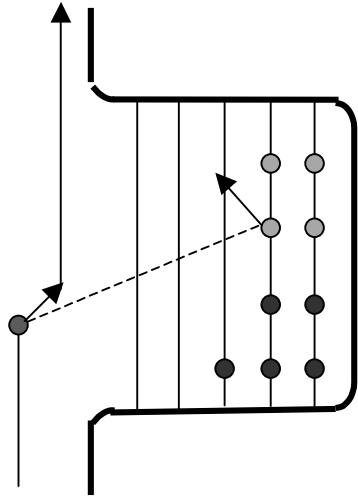
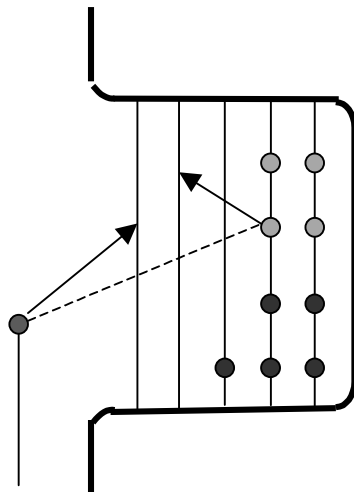


# The Optical Model



## and Direct Reactions



B.V. Carlson -- Depto. de Física

Instituto Tecnológico de Aeronáutica

São José dos Campos SP, Brazil

## Direct Reactions

- Elastic scattering –  $(n, n)$ ,  $(p, p)$ ,  $(\alpha, \alpha)$ , ...
- Inelastic Scattering --  $(n, n')$ ,  $(p, p')$ ,  $(\alpha, \alpha')$ , ...
- Knockout –  $(n, 2n)$ ,  $(n, np)$ ,  $(p, pn)$ ,  $(p, 2p)$ , ...
- Stripping –  $(d, p)$ ,  $(d, n)$ ,  $(t, d)$ , ...
- Pickup –  $(p, d)$ ,  $(n, d)$ ,  $(d, t)$ , ...
- Charge exchange –  $(n,p)$ ,  $(p,n)$ ,  $(t, {}^3\text{He})$ ,  $({}^3\text{He}, t)$ , ...

The optical model is particularly important for the study of the direct (fast) contribution to the first two of these -- elastic and inelastic scattering -- on which we will concentrate our attention.

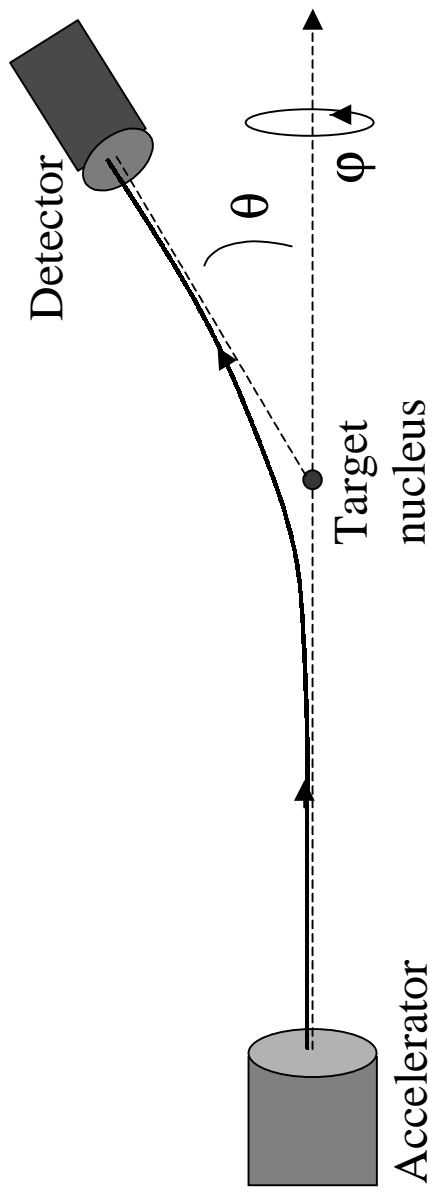
However, it also plays an important role in the analysis of the statistical (slow) contribution to nuclear reactions.

# Conservation laws

Conservation laws are important in determining the basic characteristics of nuclear reactions.

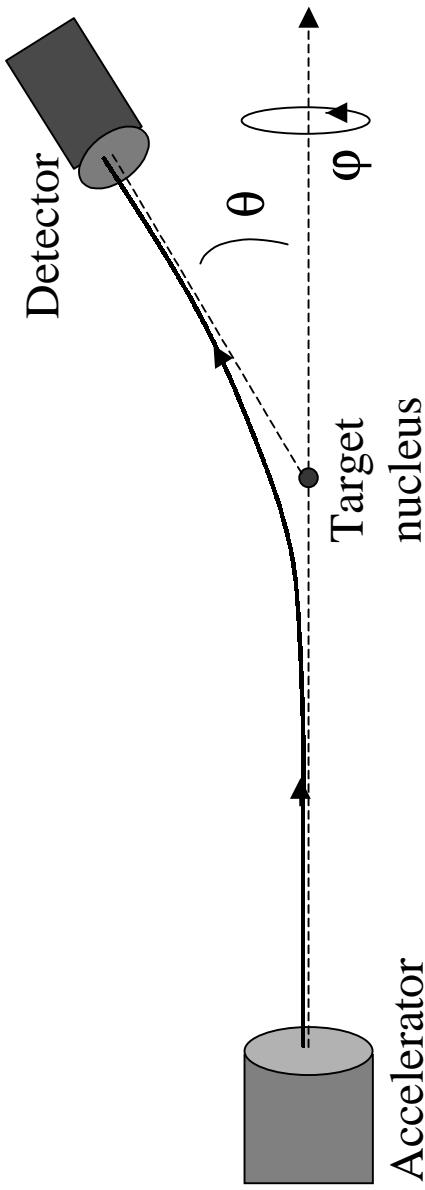
- Charge and nucleon number,  $Z$  and  $A$  --  $^{56}\text{Fe} (\text{p}, \text{n}) ^{56}\text{Co}$
- Energy,  $E - 238\text{U}(\text{n}, \text{n}')^{238}\text{U}^*$  ( $E_x = 0.045 \text{ MeV}$ )
- Linear momentum,  $\vec{p}$  – thresholds, recoil
- Angular momentum and parity,  $\vec{J}$  and  $\pi$  --  $d\sigma/d\Omega$

# Experimental Setup for Studying Scattering



- Distance from accelerator to target and from target to detector on the order of a meter or more.
- Cross sectional area of beam  $A$  on the order of  $\text{mm}^2$ .
- Target thickness  $t$  on the order of  $\mu\text{m}$  or more.
- Beam intensity –  $n_0$  (particles/s) – varies greatly, from about  $10^5$  to  $10^{13}$
- In target, atomic dimension on the order of  $10^{-10}$  m and nuclear dimension on the order of  $10^{-15}$  m.

# The Experimental Cross Section

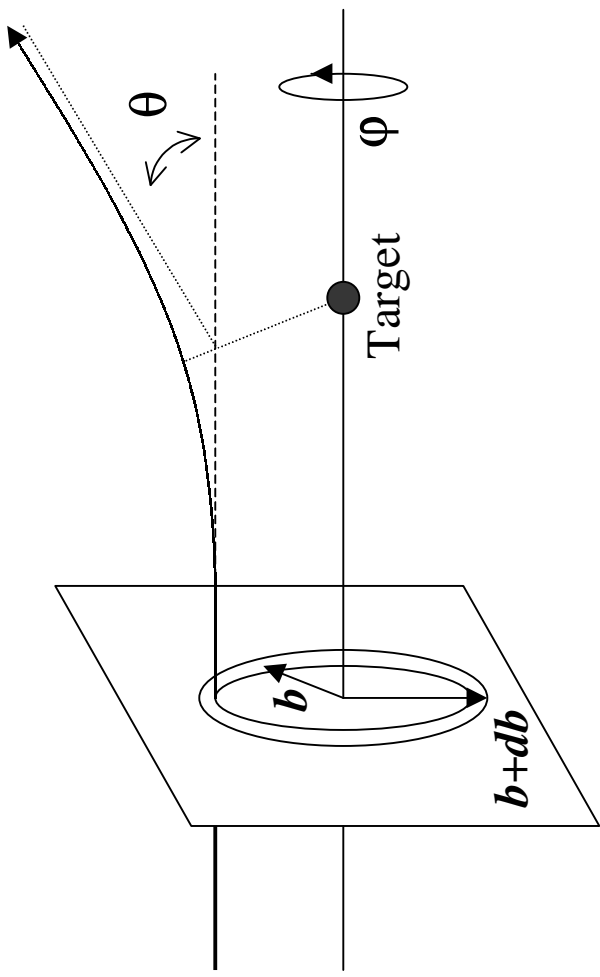


- $A$  – cross sectional area of beam
- $n_0$  – incident beam intensity
- $n(\theta, \phi)d\Omega$  -- particle intensity (part./s) entering detector of solid angle  $d\Omega$
- $\rho_{tar}$  – target particle density
- $t$  – target thickness

$$d\sigma = \frac{\text{particle intensity entering detector in solid angle } d\Omega}{(\text{incident intensity/area}) * (\text{no. of target particles in beam})} = \frac{n(\theta, \phi)d\Omega}{(n_0 / A)(\rho_{tar} tA)}$$

The differential cross section  $\frac{d\sigma}{d\Omega}$  has the units of area/solid angle.

# The Classical Cross Section



- the impact parameter
- perpendicular distance between particle trajectory and center of target

Assuming no dependence on  $\phi$ ,

$$\frac{d\sigma}{d\theta} = 2\pi b(\theta) \left| \frac{db}{d\theta} \right|$$

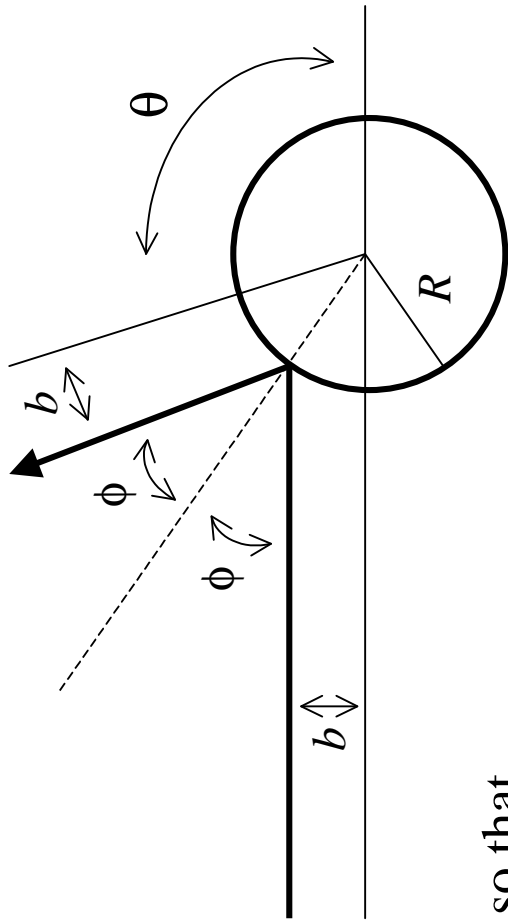
Since

$$\frac{d\sigma}{d\Omega} = \frac{b(\theta)}{\sin \theta} \left| \frac{db}{d\theta} \right|$$

↑

$$d\Omega = 2\pi \sin \theta \, d\theta$$

## An example – Hard sphere scattering



We have

$$b(\phi) = R \sin \phi$$

and

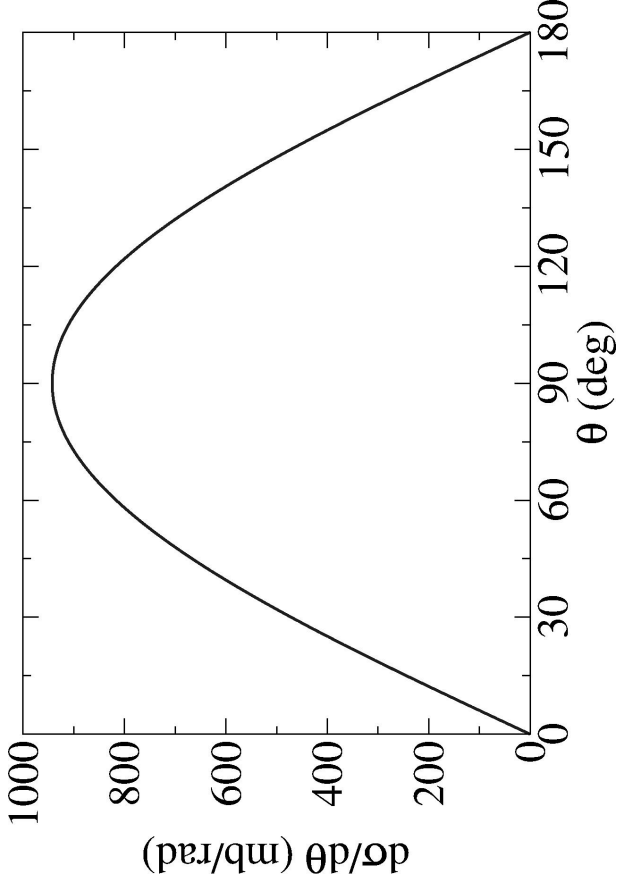
$$\phi = \frac{\pi - \theta}{2}.$$

so that

$$\frac{d\sigma}{d\theta} = 2\pi b(\theta) \left| \frac{db}{d\theta} \right| = \frac{\pi R^2}{2} \sin \theta$$

and

$$\frac{d\sigma}{d\Omega} = \frac{b(\theta)}{\sin \theta} \left| \frac{db}{d\theta} \right| = \frac{R^2}{4}$$



For  $^{238}\text{U}$ ,  $R \approx 7.5$  fm and

$$R^2/4 \approx 14 \text{ fm}^2 = 140 \text{ mb.}$$

## Another example – a sticky hard sphere

Now, suppose that a fraction of the incoming particles do not scatter, but instead stick to the target. Let us assume, for instance, that the fraction

$$P(\theta) = \alpha \cos \phi = \alpha \sin \frac{\theta}{2}$$

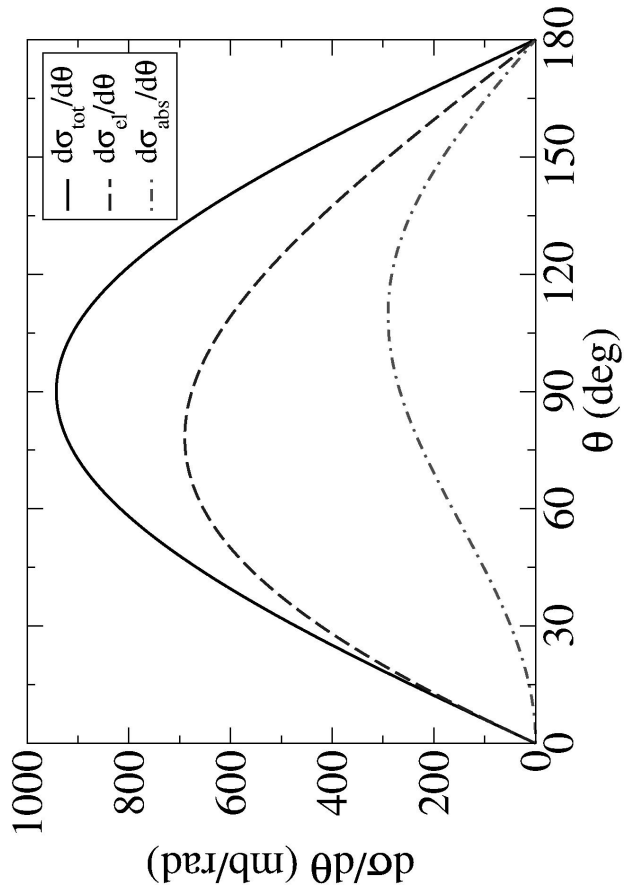
(which decreases as the collision becomes more grazing) is absorbed by the target.

Decomposition of the differential cross section:

$$\frac{d\sigma_{abs}}{d\theta} = \frac{\pi R^2}{2} P(\theta) \sin \theta$$

$$\frac{d\sigma_{el}}{d\theta} = \frac{\pi R^2}{2} (1 - P(\theta)) \sin \theta$$

$$\frac{d\sigma_{tot}}{d\theta} = \frac{d\sigma_{abs}}{d\theta} + \frac{d\sigma_{el}}{d\theta} = \frac{\pi R^2}{2} \sin \theta$$



Only  $d\sigma_{el}/d\theta$  is observed as scattered particles. In the figure,  $\alpha = 0.4$

## Integrated cross sections

We can integrate the differential cross sections over angle to obtain

$$\sigma_{abs} = \frac{\pi R^2}{2} \int_0^\pi P(\theta) \sin \theta \, d\theta = \frac{2}{3} \alpha \pi R^2$$

$$\sigma_{el} = \frac{\pi R^2}{2} \int_0^\pi (1 - P(\theta)) \sin \theta \, d\theta = \left(1 - \frac{2}{3} \alpha\right) \pi R^2$$

$$\sigma_{tot} = \sigma_{abs} + \sigma_{el} = \pi R^2$$

The total cross section of  $\pi R^2$  is what we would expect and what we would obtain in the simple hard sphere case.

In the general case, when there is a value of the impact parameter  $b_{max}$  such that  $\theta(b)=0$  for  $b>b_{max}$ , we have

$$\sigma_{tot} = 2\pi \int_0^\pi b(\theta) \left| \frac{db}{d\theta} \right| d\theta = \pi b^2 \Big|_0^{b_{max}} = \pi b_{max}^2$$

## Attenuation and the total cross section

Both elastic scattering and absorption remove particles from the incident beam. The sum of the two – the total cross section – determines how the beam is attenuated as it passes through the target.

From the definition of the cross section, we have in any

$$\sigma_{tot} = \frac{-dn}{n(z) \rho_{tar} dz}$$

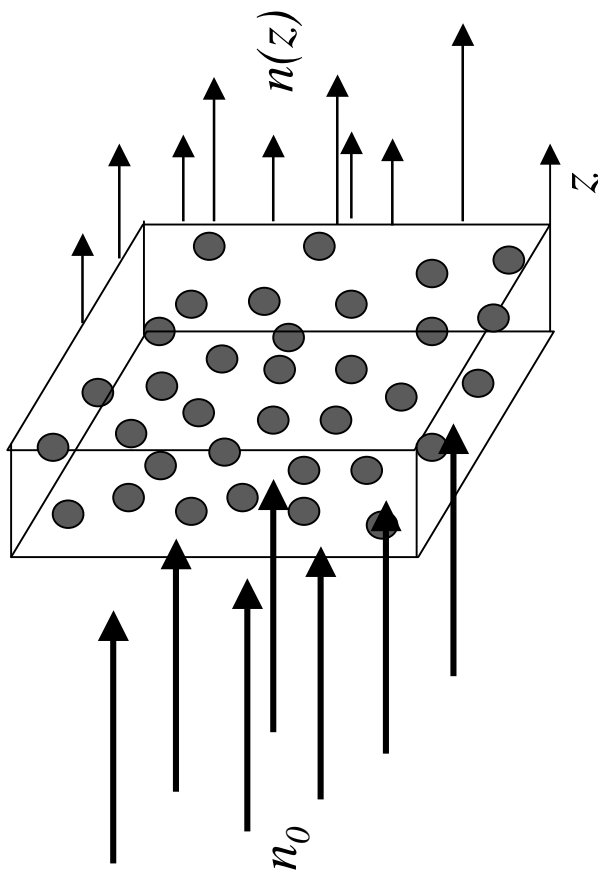
or

$$\frac{dn}{dz} = -\rho_{tar} \sigma_{tot} n(z)$$

$$\Rightarrow n(z) = n_0 \exp(-\rho_{tar} \sigma_{tot} z)$$

The inverse of the product  $\rho_{tar} \sigma_{tot}$  defines the mean free path  $\lambda$  of the projectile through the target.

$$\lambda = 1 / \rho_{tar} \sigma_{tot}$$



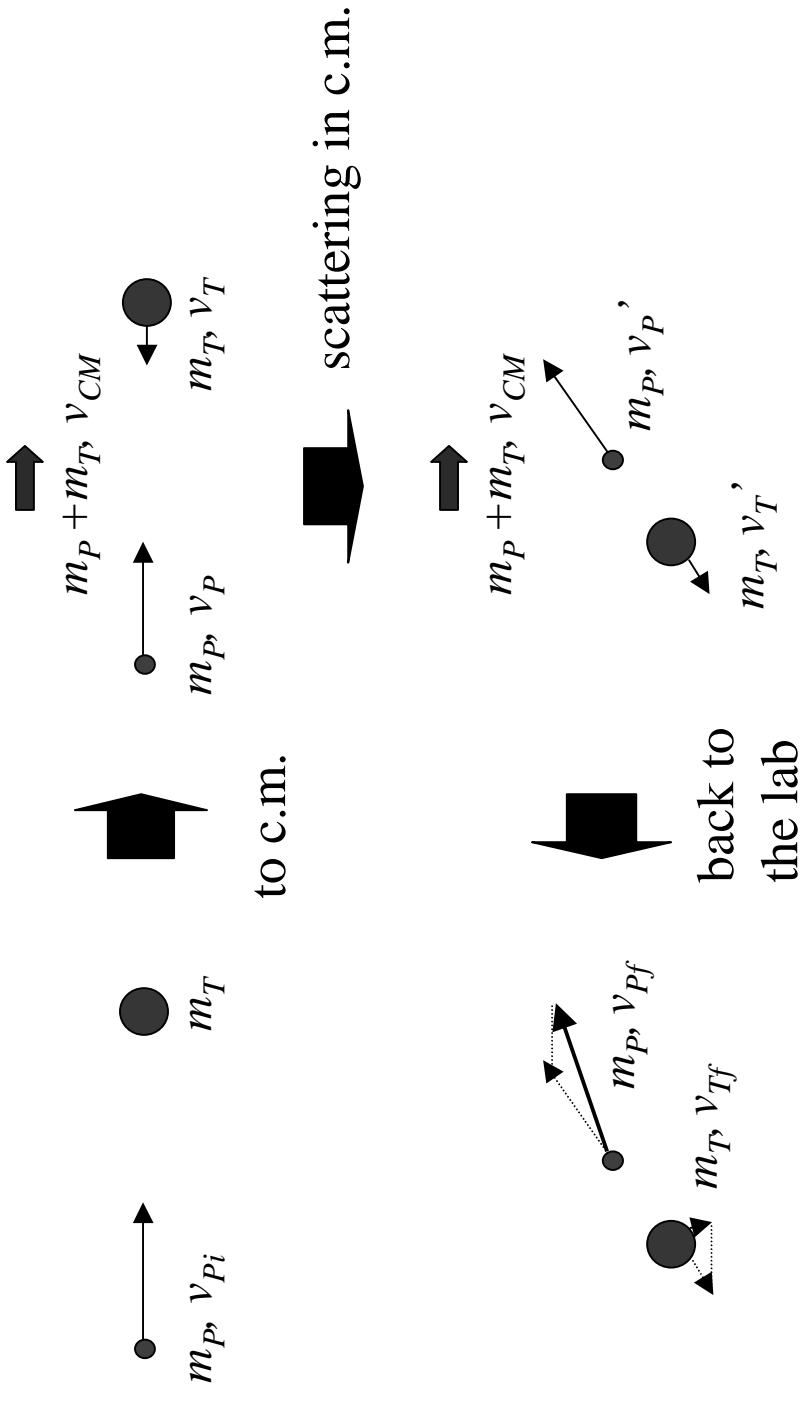
For our example of hard scattering from U-like spheres, assuming a density close to that of U, we have

$$\lambda = \left( \frac{19 * 6}{238} * 10^{29} * 177 * 10^{-30} \text{ m}^{-1} \right)^{-1} \approx 0.12 \text{ m}$$

# Laboratory and Center-of-mass Coordinates

In order to properly treat the conservation of momentum and energy, scattering problems should be analyzed in the center-of-mass frame.

The basic steps in the transformation to the center-of-mass frame and back to the lab one are shown below.



# Laboratory and Center-of-mass Coordinates - Basics

Two fundamental quantities that result from the transformation are the reduced mass  $\mu$  and the energy  $E_{cm}$  in the center-of-mass frame. In terms of the projectile and target masses,  $m_p$  and  $m_T$  and the projectile energy in the lab frame  $E_{lab}$ , these are

$$\mu = \frac{m_p m_T}{m_p + m_T} \quad \text{and} \quad E_{cm} = \frac{m_T}{m_p + m_T} E_{lab}$$

$$\text{The relative momentum in the c.m. frame is} \quad p_{cm} = \frac{m_T}{m_p + m_T} p_{lab}$$

The transformation of the scattering angle does not reduce to a simple expression. However, its numerical calculation is straightforward.

From this point on, we will assume that we are using the center-of-mass frame, unless otherwise noted.

## Yet another example – Coulomb scattering

Conservation of energy:

$$\frac{p_r^2}{2\mu} + \frac{p_{cm}^2}{2\mu} \frac{b^2}{r^2} + \frac{Z_P Z_T e^2}{r} = E_{cm}$$

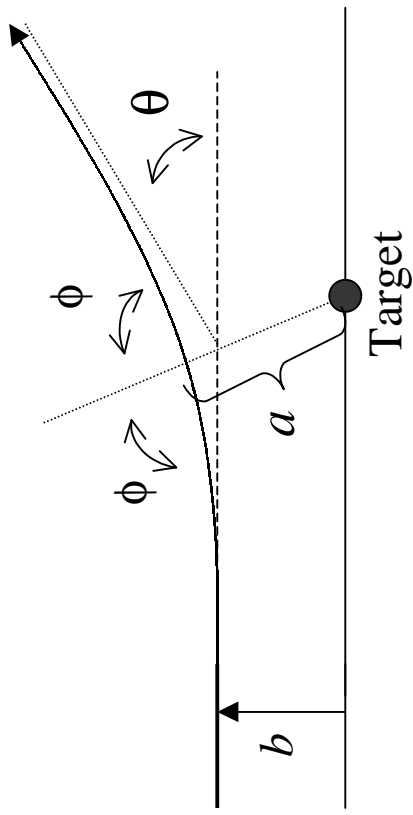
with  $p_r$  the radial momentum and  $r$  the radial coordinate and  $E_{cm} = p_{cm}^2/2\mu$ .

When  $b = 0$ , the point of closest approach  $a_0$  is given by

$$\frac{Z_P Z_T e^2}{a_0} = E_{cm} \quad \Rightarrow \quad a_0 = \frac{Z_P Z_T e^2}{E_{cm}}$$

For arbitrary  $b$ , the point of closest approach  $a$  satisfies

$$\frac{p_{cm}^2}{2\mu} \frac{b^2}{a^2} + \frac{Z_P Z_T e^2}{a} = E_{cm}$$



This becomes

$$b^2 = a(a - a_0)$$

The orbit for repulsive Coulomb scattering forms a hyperbola satisfying

$$b = a \tan\left(\frac{\phi}{2}\right)$$

Substituting in the expression above, we obtain

$$b = \frac{a_0}{2} \tan \phi$$

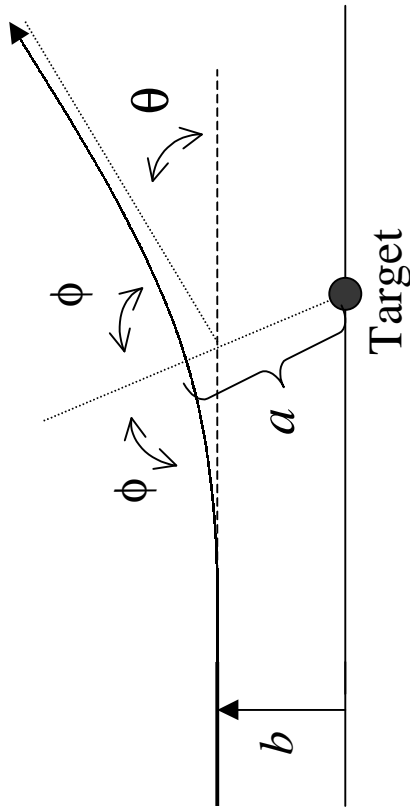
## Coulomb scattering – the differential cross section

Combining

$$\theta = \pi - 2\phi \quad \text{and} \quad b = \frac{a_0}{2} \tan \phi$$

we have

$$b = \frac{a_0}{2} \cot\left(\frac{\theta}{2}\right).$$

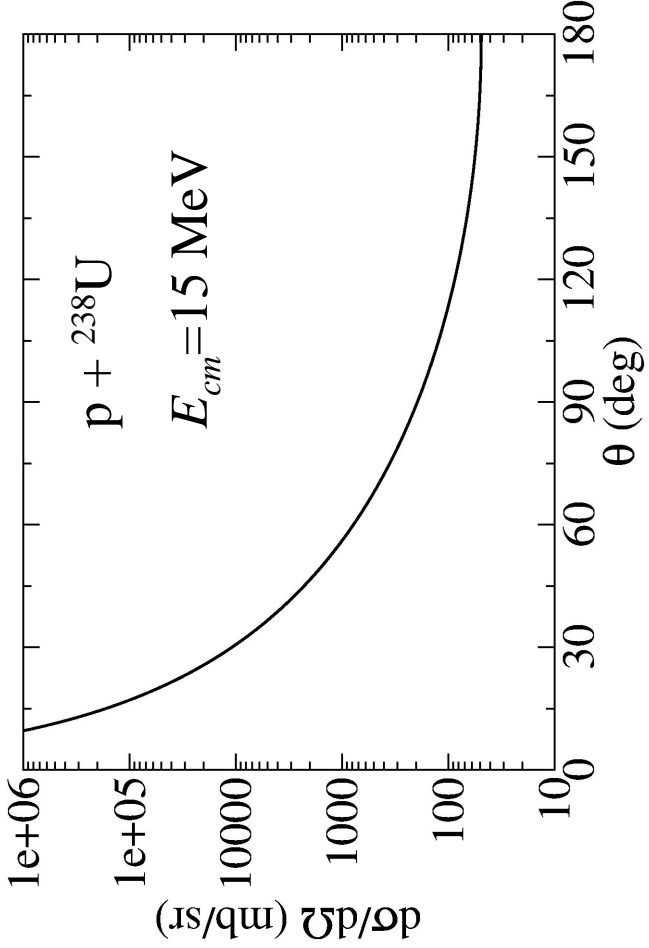


The differential cross section is then

$$\frac{d\sigma}{d\theta} = \pi \left(\frac{a_0}{2}\right)^2 \frac{\cos\left(\frac{\theta}{2}\right)}{\sin^3\left(\frac{\theta}{2}\right)}$$

or

$$\frac{d\sigma}{d\Omega} = \left(\frac{a_0}{4}\right)^2 \frac{1}{\sin^4\left(\frac{\theta}{2}\right)}.$$



## No integrated Coulomb cross section

It is obvious from its explicit form,

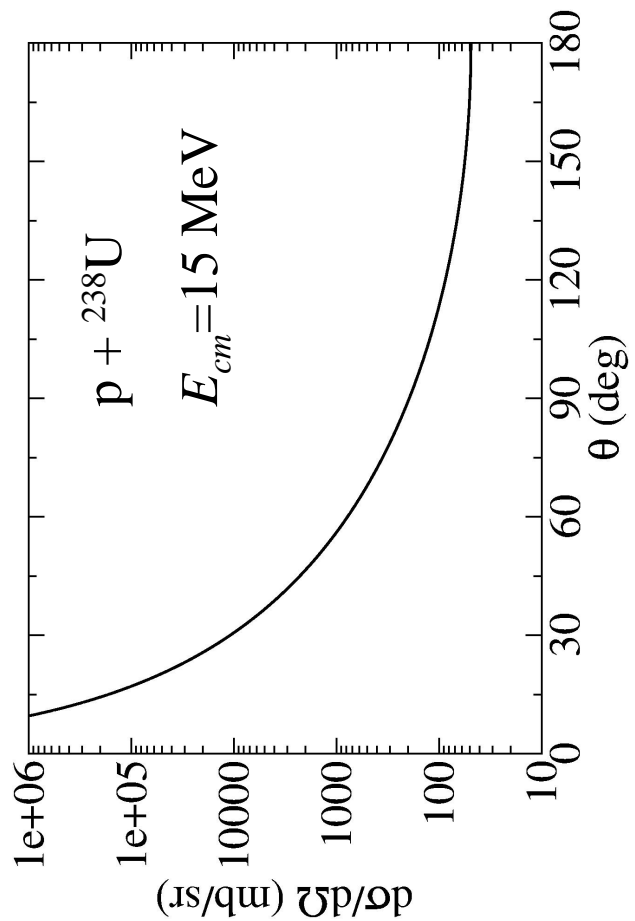
$$\frac{d\sigma}{d\Omega} = \left(\frac{a_0}{4}\right)^2 \frac{1}{\sin^4\left(\frac{\theta}{2}\right)}$$

as well as from the figure, that the Coulomb angular distribution diverges at small angles.

This expression may be integrated formally,

$$\begin{aligned} \sigma &= 2\pi \int_0^\pi \frac{d\sigma}{d\Omega} \sin \theta d\theta \\ &= \pi \left( \frac{a_0}{2 \sin(\theta/2)} \right)^2 \Big|_0^\pi \end{aligned}$$

but is also divergent.



The long range of the Coulomb potential is the physical reason for the divergences in the Coulomb angular distribution and cross section. There is no value of the impact parameter  $b_{max}$  for which scattering no longer occurs.

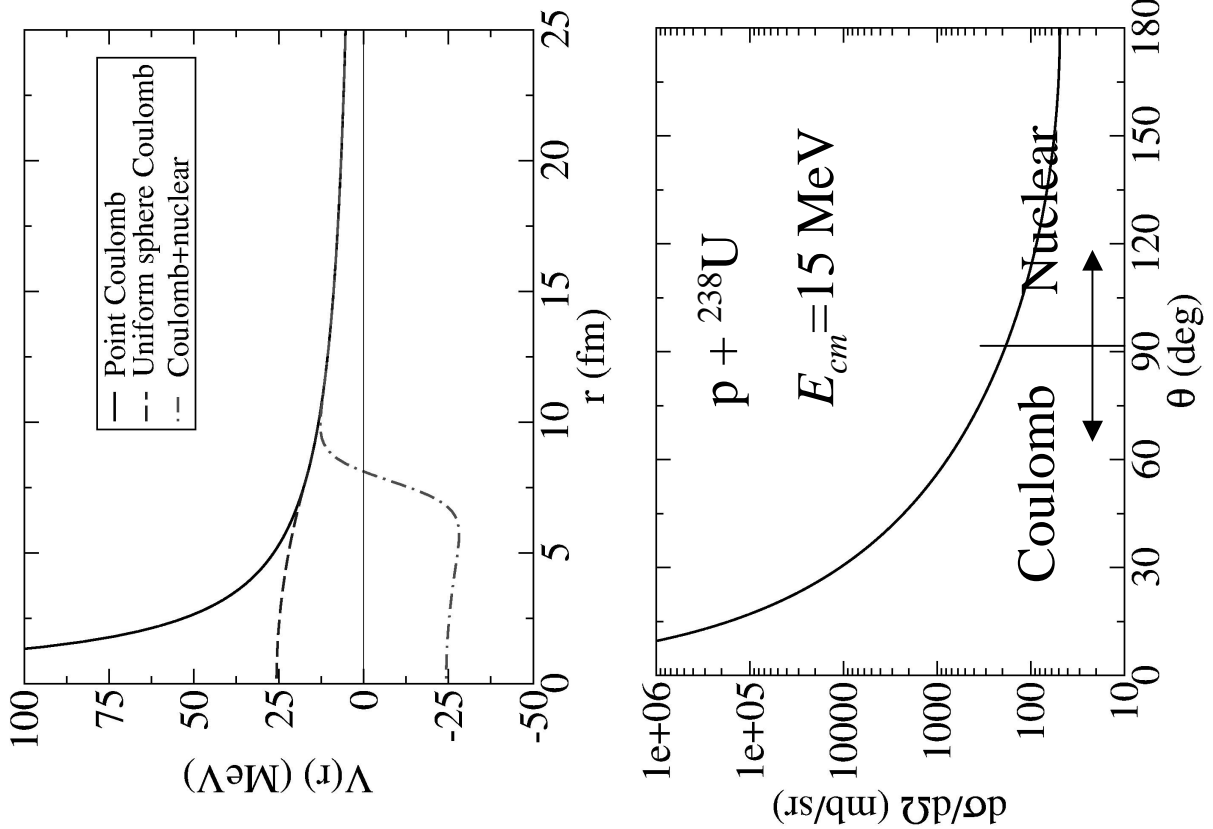
# Coulomb scattering from a charge distribution

In scattering calculations, the nuclear charge distribution is usually taken as that of a uniformly charged sphere of radius  $R_c = 1.25 * A^{1/3}$  (fm).

$$V_C(r) = \begin{cases} \frac{Z_p Z_T e^2}{2R_C} \left( 3 - (r/R_C)^2 \right) & r < R_C \\ \frac{Z_p Z_T e^2}{r} & r > R_C \end{cases}$$

Since the nuclear potential is short-ranged, the scattering at large values of the impact parameter is Coulomb scattering.

In the example given here, the scattering at angles below about  $95^\circ$  would be pure point-like Coulomb scattering.



## The Coulomb barrier for charged particles

The Coulomb + nuclear potential forms a barrier to charged particles that reaches its maximum just outside the nucleus. Outside the barrier maximum, the potential is very similar to the Coulomb potential of pointlike particles. At relative energies below the Coulomb barrier or at distances of closest approach greater than the barrier position, the scattering is almost purely point-like Coulomb scattering.

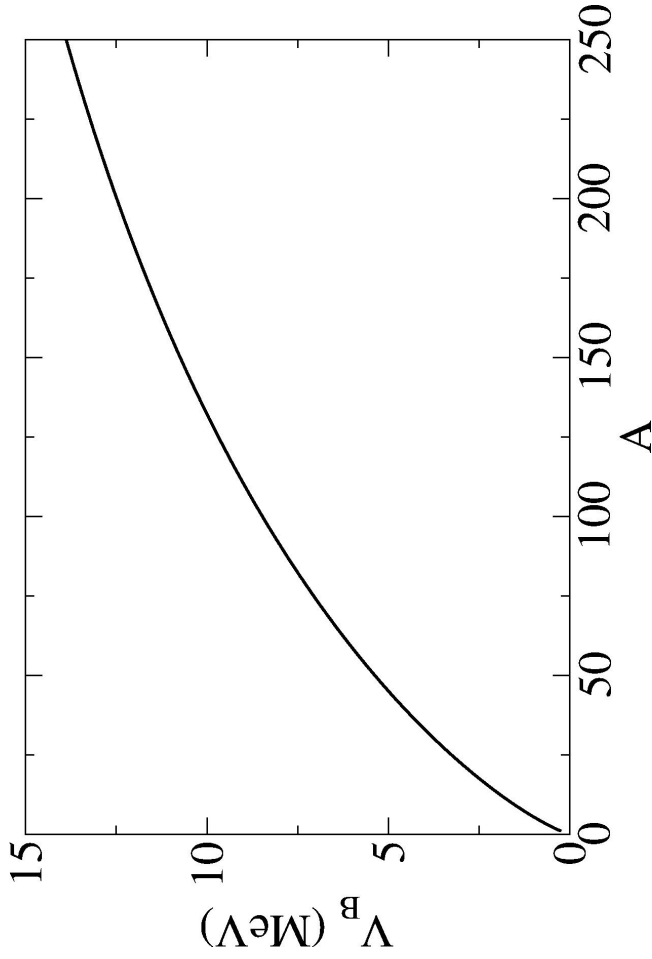
We can estimate the barrier position as

$$R_B \approx 1.25A^{1/3} + 2.0 \text{ (fm)}$$

and its height as

$$V_B \approx \frac{Z_P Z_T e^2}{R_B} \text{ (MeV).}$$

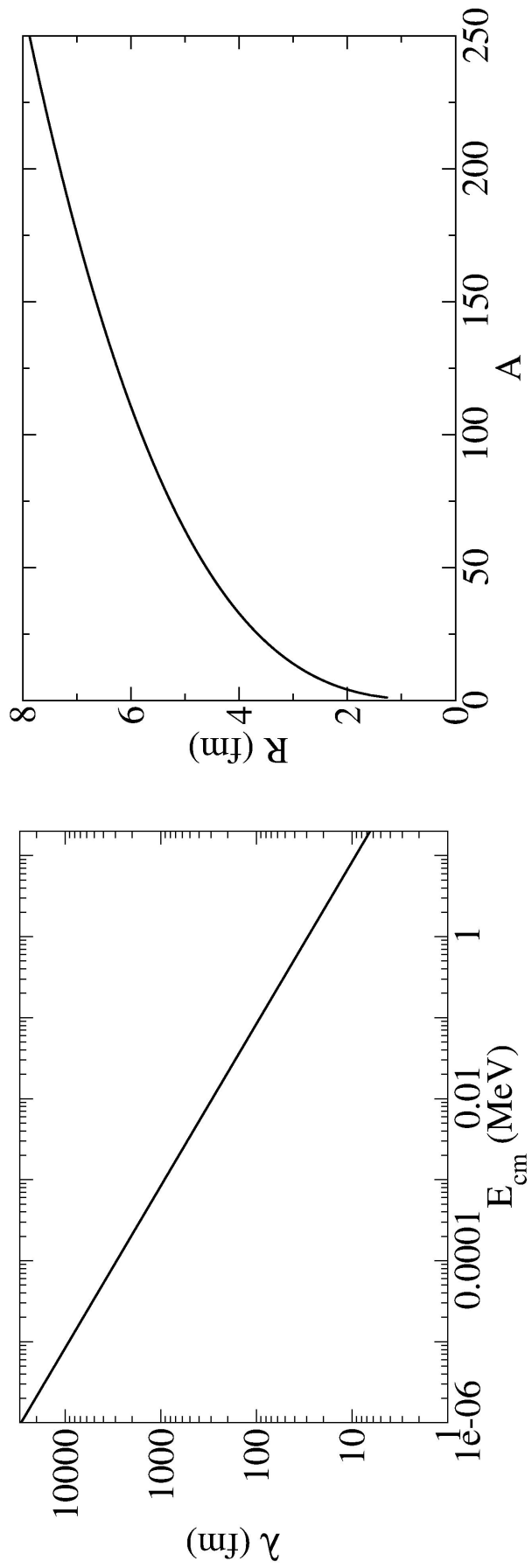
The barrier height  $V_B$  for protons is shown at the right.



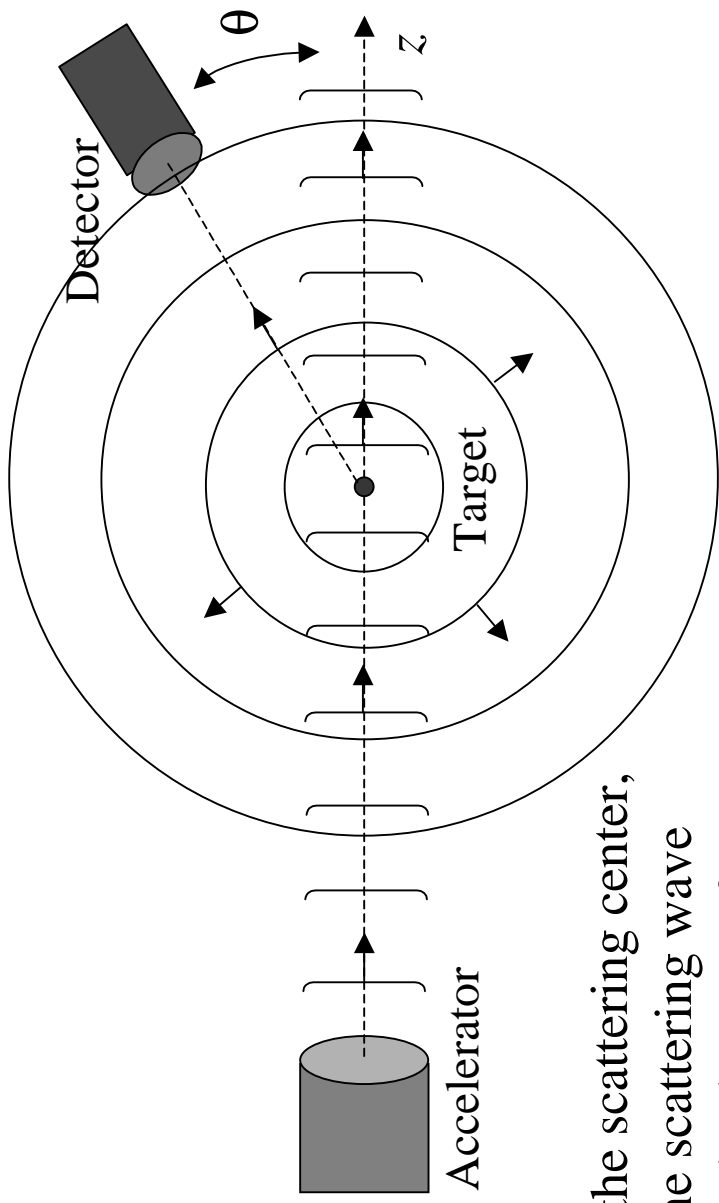
## Waves and particles

We know that the wave-like nature of the scattering particles may be neglected only if their wavelength is much smaller than the length scale on which the scattering system varies. For nuclear scattering, the appropriate length scale would be at most the size of the nucleus and should probably be of the size of the nuclear surface – about 0.5 to 1.0 fm.

Comparing the wavelength of a nucleon to a typical nuclear radius, taken to be  $R = 1.25A^{1/3}$  (fm), we find that the wavelike nature must be taken into account over the entire energy range we will consider – up to about 20 MeV.



# The quantum view of scattering



Far from the scattering center, we take the scattering wave function to be the sum of a plane wave and a scattered outgoing spherical wave,

$$\psi(\vec{r}) \approx e^{ikz} + f(\theta) \frac{e^{ikr}}{r}.$$

when  $r \rightarrow \infty$ . ( $k^2 = 2\mu E_{cm} / \hbar^2$ )

The differential cross section is the squared magnitude of the scattering amplitude,

$$\frac{d\sigma}{d\Omega} = |f(\theta)|^2.$$

## Back to the basics

We defined the differential cross section as

$$d\sigma = \frac{\text{particle intensity entering detector of solid angle } d\Omega}{(\text{incident intensity}/\text{area}) * (\text{no. of target particles in beam})} = \frac{n(\theta) d\Omega}{(n_0 / A)(\rho_{tar} tA)}$$

How did we relate this with the asymptotic form of the wave function

$$\psi(\vec{r}) \approx e^{ikz} + f(\theta) \frac{e^{ikr}}{r}. \quad \text{to obtain} \quad \frac{d\sigma}{d\Omega} = |f(\theta)|^2 ?$$

- First, we assume that we have but one target nucleus,  $\rho_{tar} tA = 1$ .
- Next, we note that  $n_0/A$  is proportional to the plane wave current density,

$$n_0 / A = \frac{\hbar}{2i\mu} \left( \psi_{in}^* \nabla \psi_{in} - (\nabla \psi_{in}^*) \psi_{in} \right) = \frac{\hbar k}{\mu} = v \quad \text{since} \quad \psi_{in} = e^{ikz}.$$

- Finally, we write the particle intensity entering the detector in terms of the current density of scattered particles,

$$n(r, \theta) d\Omega = \frac{\hbar}{2i\mu} \left( \psi_{sc}^* \partial_r \psi_{sc} - (\partial_r \psi_{sc}^*) \psi_{sc} \right) (r^2 d\Omega) \xrightarrow[r \rightarrow \infty]{} v |f(\theta)|^2.$$

# The partial-wave expansion

Neglecting spin for the moment, we use conservation of angular momentum to expand the wave function in partial waves of the orbital angular momentum,

$$\psi(r, \theta) = \sum_{l=0}^{\infty} u_l(r) P_l(\cos \theta).$$

The plane wave may be expanded as

$$e^{ikz} = \sum_{l=0}^{\infty} (2l+1)i^l j_l(kr) P_l(\cos \theta)$$

with

$$j_l(kr) = \frac{i}{2} (h_l^{(-)}(kr) - h_l^{(+)}(kr)) \quad \text{where} \quad h_l^{(\pm)}(kr) \xrightarrow[r \rightarrow \infty]{} (\mp i)^l e^{\pm ikr}.$$

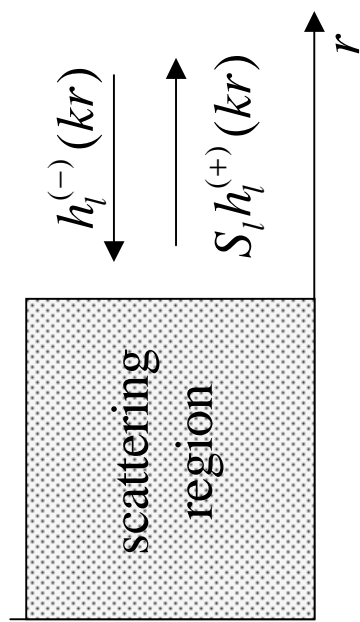
In analogy with the plane wave, we write

$$\psi(r, \theta) = \sum_{l=0}^{\infty} (2l+1)i^l \psi_l(r) P_l(\cos \theta)$$

where each of the partial waves satisfies the Schrödinger equation

$$\left( \frac{\partial^2}{\partial r^2} + k^2 - \frac{2\mu}{\hbar^2} U(r) - \frac{l(l+1)}{r^2} \right) (r \psi_l(r)) = 0.$$

## More on the partial-wave expansion



Outside the scattering region defined by the potential  $U(r)$ , the wave function  $\psi_1(\mathbf{r})$  satisfies the same Schrödinger equation as the plane wave and must be a linear combination of the same incoming / outgoing waves  $h_l^{(\pm)}(kr)$ ,

$$\psi_l(r) \rightarrow \frac{i}{2} (h_l^{(-)}(kr) - S_l h_l^{(+)}(kr)).$$

The incoming wave must be the same as that of the plane wave, so that the only difference with the plane wave is in the outgoing scattered wave.

Substituting in the partial wave expansion,

$$\begin{aligned} \psi(r, \theta) &\rightarrow \sum_{l=0}^{\infty} (2l+1)i^l \left( j_l(kr) + \frac{S_l - 1}{2i} h_l^{(+)}(kr) \right) P_l(\cos \theta) \\ &\rightarrow e^{ikz} + \frac{1}{2ik} \sum_{l=0}^{\infty} (2l+1)(S_l - 1) P_l(\cos \theta) \frac{e^{ikr}}{r}, \end{aligned}$$

so that

$$f(\theta) = \frac{1}{2ik} \sum_{l=0}^{\infty} (2l+1)(S_l - 1) P_l(\cos \theta) = \frac{4\pi}{2ik} \sum_{lm} (S_l - 1) Y_{lm}(\hat{r}) Y_{lm}^*(\hat{k}).$$

# Solving the scattering problem

How do we obtain the asymptotic form of the wave function,

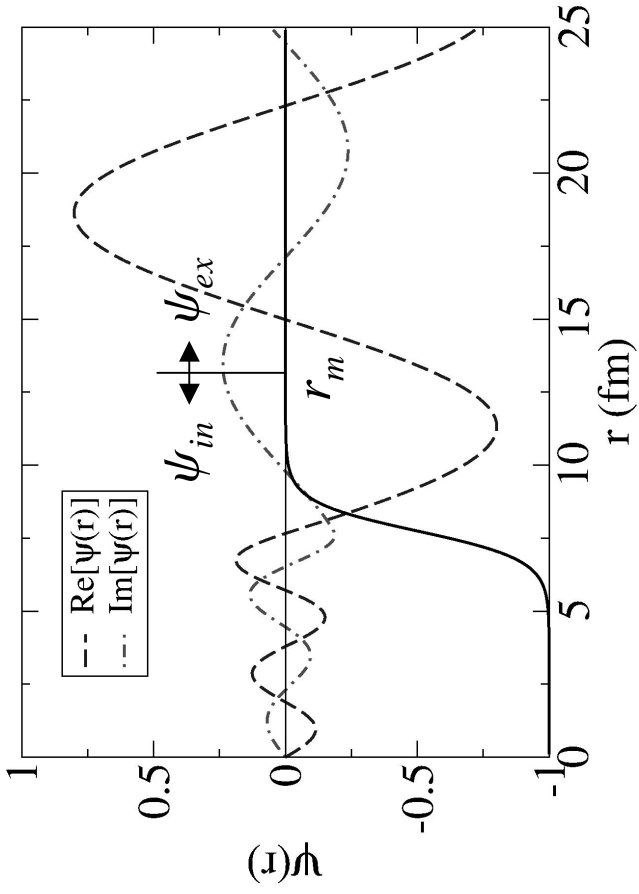
$$\psi_l(r) \rightarrow \frac{i}{2} \left( h_l^{(-)}(kr) - S_l h_l^{(+)}(kr) \right)$$

First, we fix a radius  $r_m$ , called the matching radius, that is beyond the range of the interaction.

The wave function inside the matching radius,  $\psi_{in}$ , is determined numerically, up to a multiplicative factor. Outside the matching radius, the wave function has the asymptotic form,

$$\psi_{l,ex}(r) = \frac{i}{2} \left( h_l^{(-)}(kr) - S_l h_l^{(+)}(kr) \right).$$

We require continuity of the wave function and its derivative at the matching radius.



This gives us two equations in two unknowns,  $A_l$  and  $S_l$ ,

$$A_l \psi_{l,in}(r_m) = \frac{i}{2} \left( h_l^{(-)}(kr_m) - S_l h_l^{(+)}(kr_m) \right)$$

and the derivative equation. We solve these for each value of  $l$ , stopping when  $S_l$  is sufficiently close to one.

## Integrated cross sections

We obtain the elastic cross section by integrating over the differential one,

$$\sigma_{el} = 2\pi \int_0^\pi |f(\theta)|^2 \sin \theta d\theta = \frac{\pi}{k^2} \sum_{l=0}^{\infty} (2l+1) |S_l - 1|^2.$$

We may calculate the absorption cross section by taking into account all of the flux entering and leaving the scattering region. Integrating the flux over a sphere whose radius tends to infinity, we have

$$\sigma_{abs} = -\frac{1}{V} \oint_S \vec{j} \cdot d\vec{S} = \frac{\pi}{k^2} \sum_{l=0}^{\infty} (2l+1) (1 - |S_l|^2).$$

The total cross section takes into account all flux lost from the incident plane wave, either by scattering or absorption,

$$\sigma_{tot} = \sigma_{el} + \sigma_{abs} = \frac{2\pi}{k^2} \sum_{l=0}^{\infty} (2l+1) (1 - \operatorname{Re} S_l).$$

The total cross section satisfies the optical theorem,

$$\sigma_{tot} = \frac{4\pi}{k} \operatorname{Im} f(\theta = 0^\circ).$$

## Low-energy neutron scattering – a simple example

Because of the Coulomb barrier, only neutral particles can reach the nucleus in a low-energy scattering. At extremely low energies, the centripetal barrier keeps all but  $l=0$ , s-waves away from the nucleus.

Let us re-examine hard-sphere scattering in the case of low-energy neutron scattering.

Scattering from the hard sphere requires that the wave-function vanish at the radius of the sphere. The s-wave wave function is then

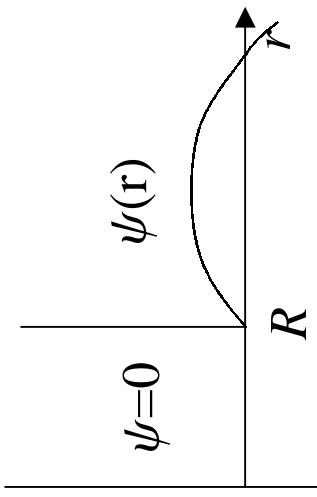
$$\psi_0(r) = \frac{i}{2kr} (e^{-ikr} - e^{-2ikR} e^{ikr}).$$

The S-matrix element is  $S_0 = e^{2ikR}$ .

The elastic cross section is

$$\sigma_{el} = 4\pi \frac{d\sigma}{d\Omega} = \frac{\pi}{k^2} |e^{-2ikR} - 1|^2.$$

This is 4 times the classical cross section.

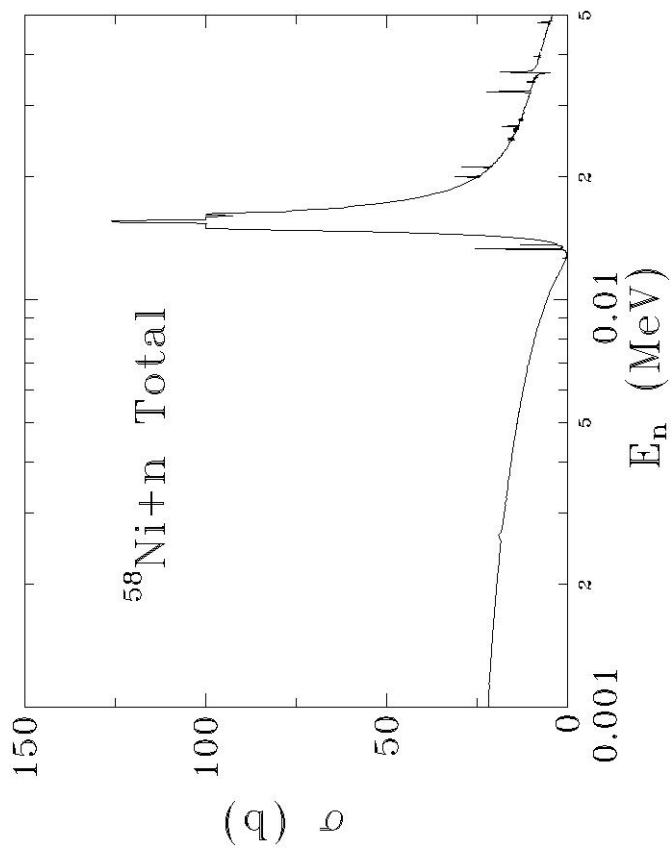


When  $k \rightarrow 0$ , the elastic cross section tends to a constant,

$$\sigma_{el} \xrightarrow{k \rightarrow 0} 4\pi R^2.$$

## Low-energy neutron scattering -- resonances

Although the neutron-nucleus interaction is attractive, its rapid variation at the nuclear surface has the same effect on low energy neutrons as a hard-sphere does— the neutrons are reflected. Absorption also usually occurs, so that the total cross section is larger than the elastic one. However, if both the elastic scattering and absorption are prompt processes, one would expect them to vary slowly with energy. Behavior of this type can be seen on the low energy side of the figure.



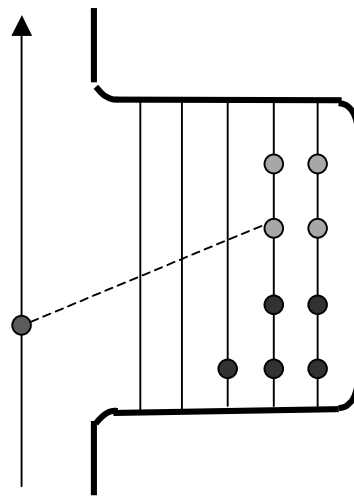
The cross section of the figure also possesses a rapidly varying resonant component, a feature common to all low-energy neutron-nucleus systems.

The resonant contribution arises from scattering through a quasi-bound state (a compound nuclear state) of the neutron+nucleus.

# Direct and compound nuclear scattering

At low energies, neutron-nucleus scattering occurs either directly or through the quasi-bound compound nucleus states.

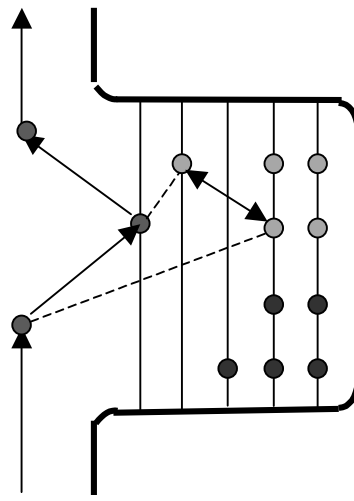
Direct scattering



$$\Delta E \Delta t \geq \hbar$$

$$\Delta t \sim 10^{-20} - 10^{-22} \text{ s}$$

Compound nuclear scattering



$$\Delta t \sim 10^{-12} - 10^{-20} \text{ s}$$

In a direct scattering, the incident neutron interacts with the average field of the nucleus. The duration of the collision is approximately the time it takes the neutron to cross the nucleus.

In a compound nuclear scattering, the incident neutron loses energy upon colliding with the nucleus and is trapped. After a fairly long interval, enough energy is again concentrated on one neutron to allow it to escape.

# Formalities - I

To formally separate the direct and compound nucleu contributions, we assume that we can partition the space of states into two components:

$\mathcal{P}$  -- containing the continuum states, such as the  $n + {}^{58}\text{Ni}$  ones, and

$\mathcal{Q}$  -- containing the quasi-bound states, such as the ground and excited states of  ${}^{59}\text{Ni}$  (and any other states that we don't want in  $\mathcal{P}$ ).

We define projection operators,  $P$  and  $Q$ , onto the subspaces with the properties

$$\begin{aligned} P^\dagger &= P & Q^\dagger &= Q, \\ P^2 &= P & Q^2 &= Q, \\ P + Q &= 1 \end{aligned}$$

We then decompose the wave function into  $\Psi = P\Psi + Q\Psi$ , where  $P\Psi$  is the continuum component and  $Q\Psi$  the quasi-bound component of the wave function.

## Formalities - II

Using P and Q, we decompose the Schrödinger equation,  $(E - H)\Psi = 0$ , into coupled equations for the two components of the wave function,

$$(E - H_{PP})P\Psi = V_{PQ}Q\Psi$$

and

$$(E - H_{QQ})Q\Psi = V_{QP}P\Psi,$$

where

$$H_{PP} \equiv PH_0P + PVP, \quad V_{PQ} \equiv PHQ = PVQ, \quad \text{etc.,}$$

and we have assumed that the contributions of the kinetic energy and the target Hamiltonian, both contained in  $H_0$ , do not couple the  $\mathcal{P}$  and  $Q$  subspaces.

We can now solve the second equation formally, using an outgoing wave boundary condition, to obtain  $Q\Psi$ ,

$$Q\Psi = (E^{(+)} - H_{QQ})^{-1}V_{QP}P\Psi$$

and substitute in the first of these to obtain an equation for  $P\Psi$  alone,

$$(E - H_{PP} - V_{PQ}(E^{(+)} - H_{QQ})^{-1}V_{QP})P\Psi = 0,$$

and which explicitly contains the direct and compound processes we expect.

## Formalities - III

However, it will be useful for us to follow a more convoluted path here. We first solve for the continuum component of the wave function  $P\Psi$ ,

$$P\Psi_c = \phi_c^{(+)} + (E^{(+)} - H_{PP})^{-1} V_{PQ} Q\Psi_c,$$

where the wave function  $\phi_c^{(+)}$  satisfies the equation

$$(E - H_{PP})\phi_c^{(+)} = 0,$$

with an incoming wave in channel c. When the solution for  $P\Psi$  is substituted in the equation for  $Q\Psi$ , the latter may be rewritten as

$$(E - H_{QQ} - W_{QQ})Q\Psi_c = V_{QP}\phi_c^{(+)},$$

where

$$W_{QQ} \equiv V_{QP}(E^{(+)} - H_{PP})^{-1} V_{PQ}.$$

In the last expression, we may decompose the  $\mathcal{P}$ -subspace propagator as

$$\frac{1}{E^{(+)} - H_{PP}} = \frac{P.P.}{E - H_{PP}} - i\pi\delta(E - H_{PP})$$

where P.P. is the principal part. The open channels in the  $\mathcal{P}$  subspace make a negative imaginary contribution to  $W_{QQ}$ , leading to poles of the the wave function in the lower half of the complex energy plane.

## Formalities - IV

If we solve the equation for  $Q$ -subspace component,

$$(E - H_{QQ} - W_{QQ})Q\Psi_c = V_{QP}\phi_c^{(+)} \quad \rightarrow \quad Q\Psi_c = (E - H_{QQ} - W_{QQ})^{-1}V_{QP}\phi_c^{(+)},$$

we may substitute this in the solution for the  $\mathcal{P}$ -subspace component,

$$P\Psi_c = \phi_c^{(+)} + (E^{(+)} - H_{PP})^{-1}V_{PQ}Q\Psi_c,$$

to immediately obtain,

$$P\Psi_c = \phi_c^{(+)} + (E^{(+)} - H_{PP})^{-1}V_{PQ}(E - H_{QQ} - W_{QQ})^{-1}V_{QP}\phi_c^{(+)}. \quad \text{.}$$

This is a solution for the complete  $\mathcal{P}$ -subspace wave function in terms of pure continuum component  $\phi_c^{(+)}$  and a compound nucleus component.

The prompt contribution of  $V_{PP}$  to the scattering is not as visible as before – it is contained in the wave function  $\phi_c^{(+)}$  and in the  $\mathcal{P}$ -subspace propagator. The compound nucleus term appears in a modified form, in which passage through the continuum is taken into account by the  $W_{QQ}$  term in the  $Q$ -subspace propagator.

## Low-energy neutron scattering -- resonances

We may now take the expression for the  $\mathcal{P}$ -subspace wave function,

$$P\Psi_c = \phi_c^{(+)} + (E^{(+)} - H_{PP})^{-1} V_{PQ} (E - H_{QQ} - W_{QQ})^{-1} V_{QP} \phi_c^{(+)},$$

and apply it to s-wave neutron scattering, for which,

$$\Psi_0(r) = \frac{i}{2kr} (e^{-ikr} - S_0 e^{ikr}),$$

outside the range of the interaction. (We continue to neglect the spin of the neutron.)

After a bit of work, we can approximate the S-matrix of the  $\mathcal{P}$ -subspace wave function in a multi-level Breit-Wigner form (among others) as

$$S_{0,ab} = e^{-i(\phi_a + \phi_b)} \left( \delta_{ab} - i \sum_{\mu} \frac{g_{\mu a} g_{\mu b}}{E - \varepsilon_{\mu} + i\Gamma_{\mu}/2} \right),$$

where  $\phi_a$  and  $\phi_b$  are the initial and final channel phase shifts and  $g_{\mu c}$  characterizes the coupling of the compound state  $\mu$  to the continuum channel  $c$ , with  $\Gamma_{\mu} = \sum_c g_{\mu c}^2$ .

The phase shifts vary slowly with the energy while the resonance sum varies quickly.

## Low-energy neutron scattering – cross sections

The cross sections directly related to the elastic S-matrix element are the elastic, absorption and total ones,

$$\sigma_{el} = \frac{\pi}{k^2} |S_{0,aa} - 1|^2, \quad \sigma_{abs} = \frac{\pi}{k^2} (1 - |S_{0,aa}|^2),$$

and

$$\sigma_{tot} = \sigma_{el} + \sigma_{abs} = \frac{2\pi}{k^2} (1 - \operatorname{Re} S_l).$$

The absorption cross section is non-zero when non-elastic channels, such as  $\gamma$  emission or fission, remove flux from the compound nucleus. The cross sections for these take the form

$$\sigma_{ac} = \frac{\pi}{k^2} |S_{0,ca}|^2.$$

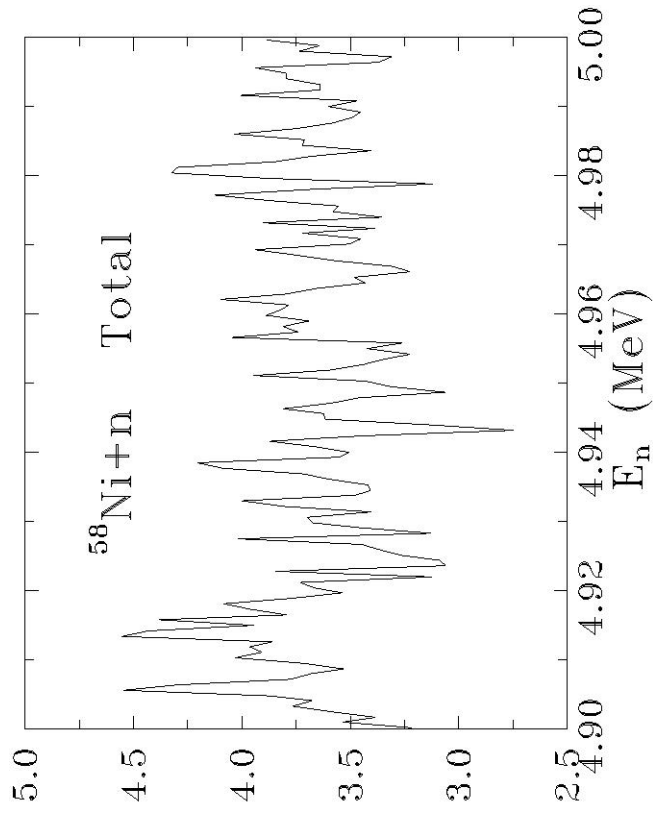
The total flux is conserved, so that

$$\sigma_{abs} = \sum_{c \neq a} \sigma_{ca} \quad \text{and} \quad \sigma_{tot} = \sigma_{el} + \sigma_{abs}.$$

The elastic cross section is well described at energies below the resonance region by a hard-sphere cross section of  $4\pi R^2$ .

# From resonances to fluctuations

At low energies, the resonance expression for the  $l=0$  S-matrix, and for higher partial waves as well, permits the separation of the direct and compound contributions to cross sections. However, the density of compound nucleus states increases rapidly with energy so that the resonances overlap and can no longer be distinguished. The cross section fluctuates rapidly, as in the figure, but the fluctuations, called Ericson fluctuations, cannot be attributed to individual resonances.



It is in this context that the optical model plays a fundamental role. The objective of the model is to describe just the prompt, direct reactions in a collision. To this end, one defines the optical potential as the potential that furnishes the energy-averaged (short time) scattering amplitudes.

## Energy averaging and the optical potential

To obtain the optical potential, we begin by calculating the energy average of the  $\mathcal{P}$ -subspace wave function, which depends linearly on the scattering amplitude. After rewriting the wave function in the form of an equation, we will obtain an expression for the optical potential.

The energy average of the  $\mathcal{P}$ -subspace wave function may be written directly,

$$\langle P\Psi_c \rangle = \phi_c^{(+)} + (E^{(+)} - H_{PP})^{-1} V_{PQ} \left\langle 1/e_{QQ} \right\rangle V_{QP} \phi_c^{(+)},$$

since the only rapidly varying quantity in the wave function is

$$e_{QQ} = E - H_{QQ} - W_{QQ}.$$

By multiplying by  $(E - H_{PP})$  as well as solving formally for  $\phi_c^{(+)}$  and substituting, we can write a Schrödinger-like equation for  $\langle P\Psi_c \rangle$ ,

$$\left( E - H_{PP} - V_{PQ} \frac{1}{\left\langle 1/e_{QQ} \right\rangle^{-1} + W_{QQ}} V_{QP} \right) \langle P\Psi_c \rangle = 0.$$

The optical potential is then

$$U_{opt} = V_{PP} + V_{PQ} \frac{1}{\left\langle 1/e_{QQ} \right\rangle^{-1} + W_{QQ}} V_{QP}$$

## Performing the energy average

To conclude the derivation of the optical potential, we must calculate  $\langle 1/e_{QQ} \rangle$ . Although there are many ways to perform the average, the simplest is to average over a normalized Lorentzian density,

$$\langle 1/e_{QQ} \rangle = \int dE_0 \frac{\rho(E, E_0)}{E_0 - H_{QQ} - W_{QQ}}$$

where

$$\rho(E, E_0) = \frac{1}{2\pi} \frac{\Delta}{(E - E_0)^2 + \Delta^2/4}.$$

Assuming that  $1/e_{QQ}$  has no poles in the upper half of the complex E plane (causality), we can perform the integral by closing the contour in the UHP to find

$$\langle 1/e_{QQ} \rangle = (E + i\Delta/2 - H_{QQ} - W_{QQ})^{-1}$$

so that

$$U_{opt} = V_{PP} + V_{PQ} \frac{1}{E - H_{QQ} + i\Delta/2} V_{QP}$$

The optical potential is energy-dependent, non-local and complex. Its imaginary part is negative, resulting in a potential that is absorptive. The absorption accounts for the flux that is lost to the  $Q$ -subspace.

## Low-energy neutron scattering – optical potential

One finds for the low-energy neutron s-wave S-matrix element  $S_0 = e^{-2ik\rho}$ , where  $\rho$  is a complex scattering length.  $R = |\rho|$  is called the scattering radius.

The resulting elastic cross section tends to a constant as the energy tends to zero, while the absorption and total cross sections diverge at small energy as  $1/k$ .

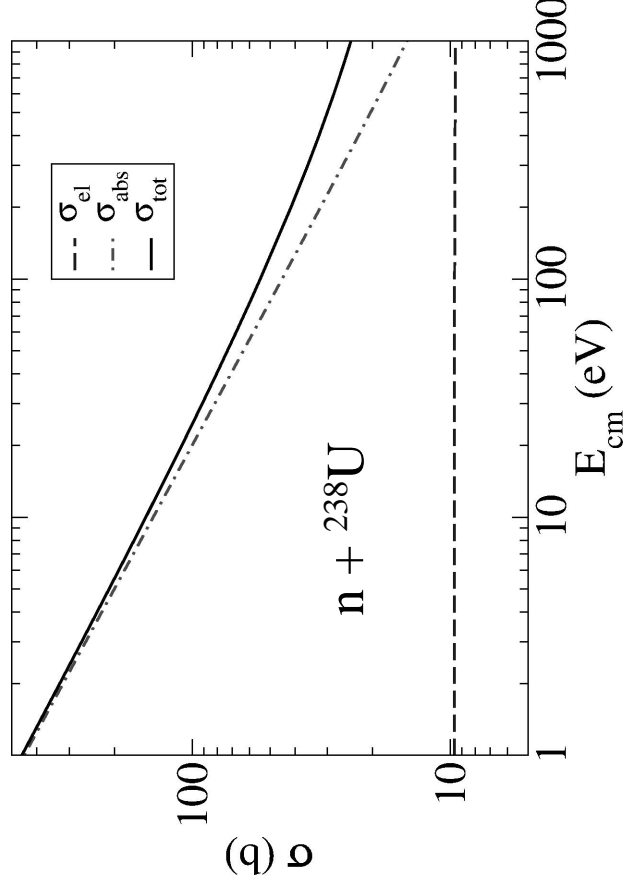
We have, as  $k \rightarrow 0$ ,

$$\sigma_{el} = 4\pi \frac{d\sigma}{d\Omega} \rightarrow 4\pi R^2,$$

$$\sigma_{abs} \rightarrow -\frac{4\pi}{k} \text{Im } \rho (1 + 2k \text{Im } \rho),$$

and

$$\sigma_{tot} = \sigma_{el} + \sigma_{abs}.$$



## Experimental significance

An optical model calculation furnishes a wave function and a scattering amplitude that should describe the prompt part of the scattering. The S-matrix that results is an energy-averaged one. We could write the S-matrix before averaging as

$$\mathfrak{S}_0 = S_0 + S_{0,fluc}, \quad \text{with} \quad \langle S_{0,fluc} \rangle = 0, \quad \text{so that} \quad \langle \mathfrak{S}_0 \rangle = \langle S_0 \rangle.$$

The energy-averaged total cross-section is just the optical one,

$$\sigma_{tot} = \frac{2\pi}{k^2} (1 - \text{Re} \langle \mathfrak{S}_0 \rangle) = \frac{2\pi}{k^2} (1 - \text{Re} S_0),$$

since it is linear in the S-matrix.

However, the energy-averaged elastic and absorption cross sections are

$$\sigma_{el} = \frac{\pi}{k^2} \langle |\mathfrak{S}_0 - 1|^2 \rangle = \frac{\pi}{k^2} |S_0 - 1|^2 + \frac{\pi}{k^2} \langle |S_{0,fluc}|^2 \rangle$$

and

$$\sigma_{abs} = \frac{\pi}{k^2} \langle 1 - |\mathfrak{S}_0|^2 \rangle = \frac{\pi}{k^2} (1 - |S_0|^2) - \frac{\pi}{k^2} \langle |S_{0,fluc}|^2 \rangle.$$

Only the total optical cross section may be compared with the experimental one.

# The S-wave strength function

If we average the resonance expression for the elastic S-matrix,

$$S_{0,aa} = e^{-2i\phi_a} \left( 1 - i \sum_\mu \frac{\Gamma_{\mu a}}{E - \varepsilon_\mu + i\Gamma_\mu / 2} \right), \quad \text{where } \Gamma_{\mu a} = g_{\mu a}^2,$$

over the Lorentzian that was used to obtain the optical potential, we find

$$\bar{S}_{0,aa} = e^{-2i\phi_a} \left( 1 - i \sum_\mu \frac{\Gamma_{\mu a}}{E - \varepsilon_\mu + i\Delta} \right) \approx e^{-2i\phi_a} \left( 1 - \frac{\pi \bar{\Gamma}_n}{D} \right),$$

where  $\bar{\Gamma}_n$  is the average neutron width and  $D$  the average s-wave resonance spacing. Since the average is the same as that of the optical potential, the average S-matrix should be the same as the optical one. In particular, we expect

$$1 - |S_0|^2 \approx 2\pi \frac{\bar{\Gamma}_n}{D}$$

when  $\bar{\Gamma}_n \ll D$ . We define the strength function as

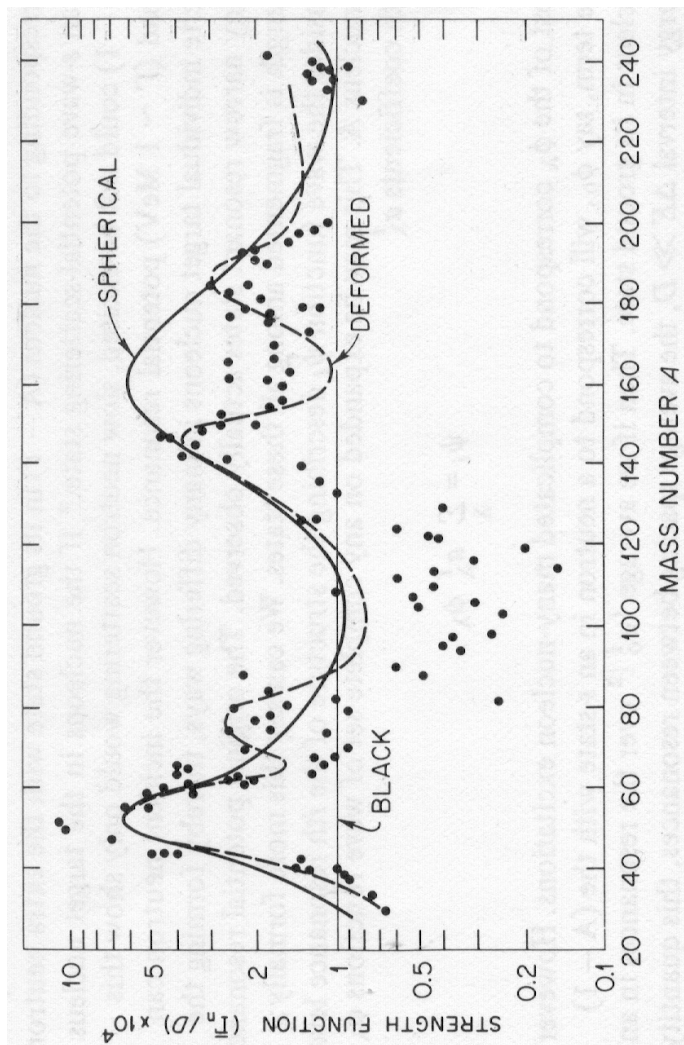
$$S_0 = \frac{\bar{\Gamma}_n}{D} \left( \frac{E_0}{E_{cm}} \right)^{1/2} \approx \frac{1}{2\pi} \left( \frac{E_0}{E_{cm}} \right)^{1/2} \left( 1 - |S_0|^2 \right)$$

where  $E_0$  is usually taken to be 1 eV. The factor of  $\sqrt{E_{cm}}$  cancels the energy dependence of the neutron partial width.

# Strength functions and SPRT

The s-wave strength function may be obtained from experimental data, either from measurements of the total cross section or from averages over resonances. When compared to optical model calculations, the agreement is quite good. The two peaks in the s-wave strength function occur in the regions where the  $3s1/2$  and  $4s1/2$  neutron shell-model orbitals are becoming bound and have a large overlap with continuum states.

A p-wave strength function may also be associated with p-wave absorption and extracted from data. The two strength functions, together with the scattering radius and the total cross section, may be used to fit optical model parameters at low energy. This is known as the SPRT method.

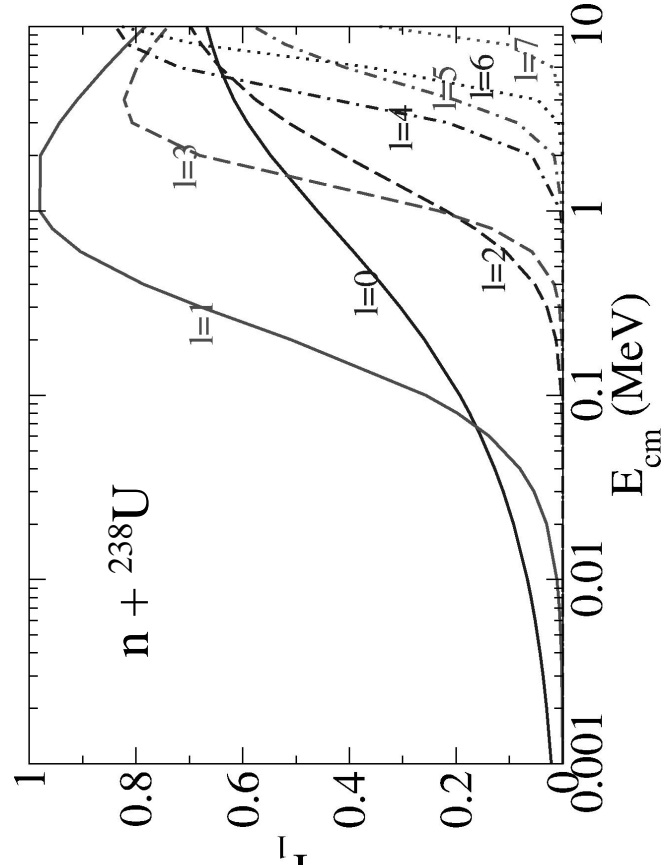
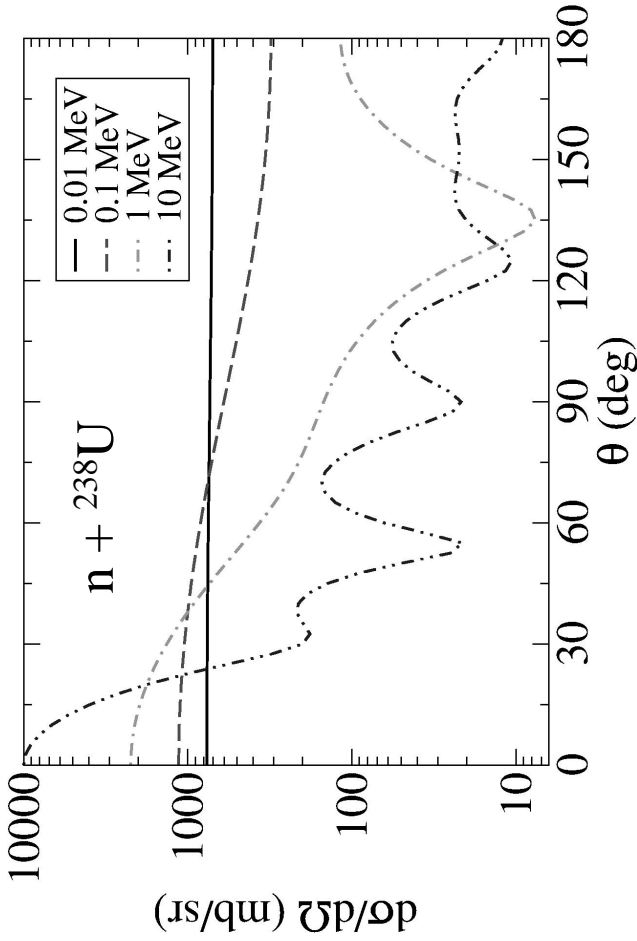


## Higher partial waves

The angular distribution for a pure s-wave is obviously constant. As the energy increases, more partial waves participate in the scattering and the angular distribution becomes more forward peaked.

The highest partial wave contributing to the scattering may be crudely estimated as  $l_{max} \approx KR$ . For  $n + {}^{238}U$  at an energy of 1 MeV, this gives  $l_{max} \approx 1.6$ .

An important auxiliary quantity determined in an optical model calculation is the transmission coefficient,  $T_l = 1 - |S_l|^2$ , which is used to calculate the fluctuating contribution to the cross sections. The transmission coefficient measures the fraction of flux that is absorbed from each partial wave.



## The partial wave expansion for charged particles

The difference between the partial wave expansion for neutral and charged particles is the long-range Coulomb potential. Rather than consider a plane wave, one must consider a Coulomb wave, which contains an additional logarithmic phase. The wave function may be expanded as

$$\psi_c = \frac{1}{kr} \sum_{l=0}^{\infty} (2l+1)i^l e^{i\sigma_l} F_l(kr) P_l(\cos\theta),$$

with

$$F_l(kr) = \frac{i}{2} \left( e^{-i\sigma_l} H_l^{(-)}(kr) - e^{i\sigma_l} H_l^{(+)}(kr) \right)$$

where the  $\sigma_l$  are the Coulomb phase shifts and

$$H_l^{(\pm)}(kr) \xrightarrow[r \rightarrow \infty]{} (\mp i)^l e^{\pm i(kr - \eta \ln 2kr)} \quad \text{with} \quad \eta = ka_0.$$

One may proceed as before to extract the scattering amplitude as

$$f(\theta) = f_c(\theta) + \frac{1}{2ik} \sum_{l=0}^{\infty} (2l+1)e^{2i\sigma_l} (S_l - 1) P_l(\cos\theta).$$

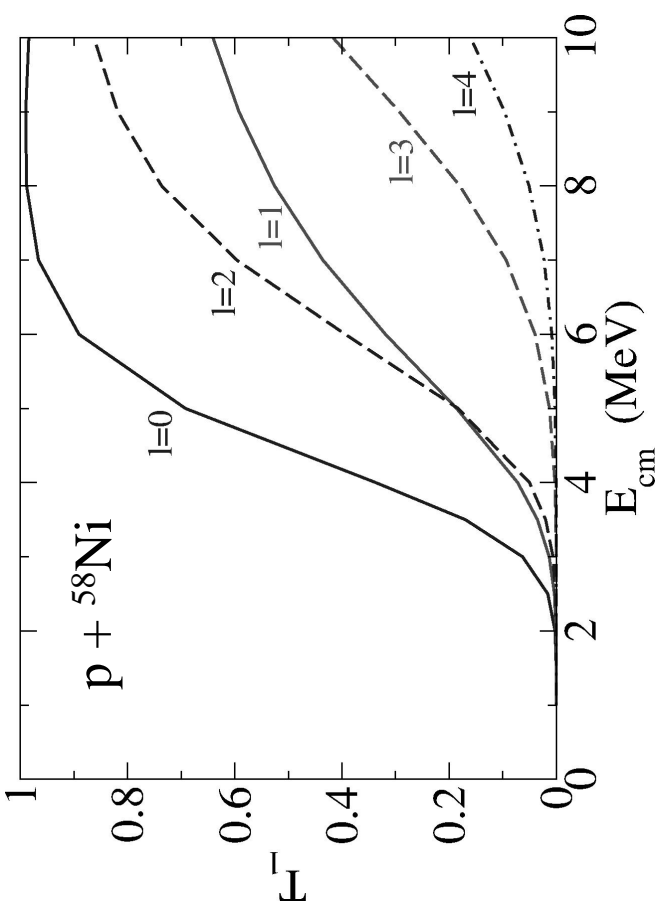
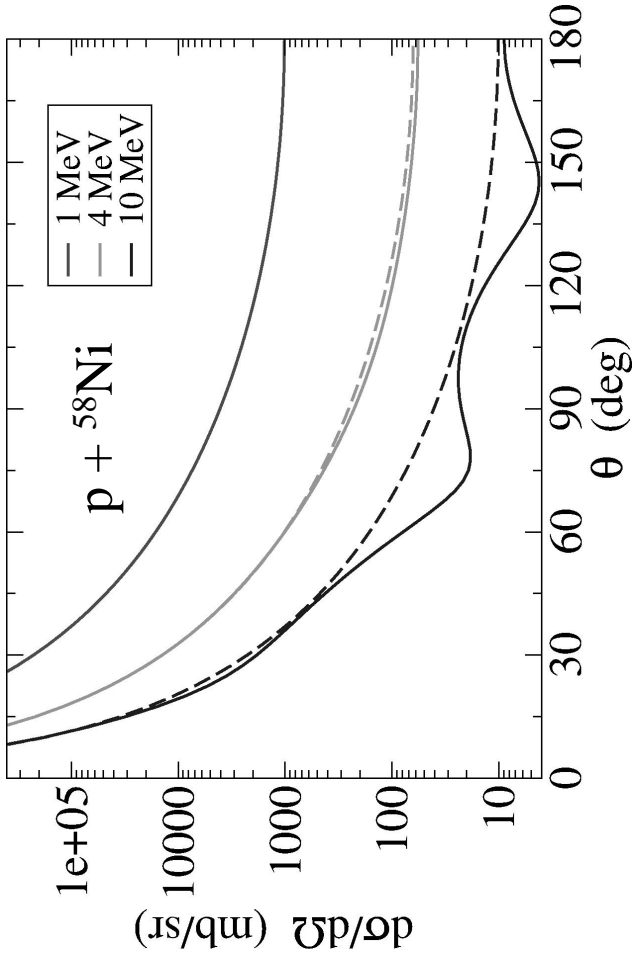
where

$$f_c(\theta) = -\frac{\eta}{2k \sin^2 \theta / 2} \exp \left[ -i\eta \ln \left( \sin^2 \theta / 2 \right) + 2i\sigma_0 \right].$$

The quantum Coulomb scattering cross section is identical to the classical one.

## Proton scattering

The angular distribution for proton scattering on  $^{58}\text{Ni}$  at 1 MeV is a pure Coulomb one. Even at 4 MeV, the difference from the pure Coulomb angular distribution appears small. At 10 MeV, substantial deviations have appeared.



Nuclear effects are more easily distinguished in the transmission coefficients. They support the observation that the scattering is purely Coulomb at 1 MeV. However, at 4 MeV, 40% of the s-wave and about 10% of the p- and d-wave have been absorbed. Angular momenta through  $l=4$  contribute at 10 MeV.

# The optical potential

We obtained a formal expression for the optical potential,

$$U_{opt} = V_{PP} + V_{PQ} \frac{1}{E - H_{QQ} + i\Delta/2} V_{QP}$$

by rewriting the energy-average of the continuum component of the wave function as an equation for itself. We observed that this potential is complex, non-local and energy-dependent.

A good deal of work has been done to calculate the optical potential from first principles. These potentials are usually non-local, except at very high energies, which tends to complicate their use.

Phenomenological optical potentials are normally used to fit and compare with experimental data. These potentials are usually taken to be local. However, their geometrical characteristics and the general trend of their energy dependence are quite similar to those of microscopic potentials. They can furnish insight into what one should expect of a microscopic potential. After all, both potentials are trying to describe the same physical processes.

# The phenomenological optical potential

Empirical optical potentials are determined by adjusting a limited set of parameters to the data on hand. Over the years, a standard form of the potential has evolved, which permits the parametrization of the scattering of most light particles ( $n$ ,  $p$ ,  $d$ ,  $t$ ,  $^3\text{He}$ , or  $\alpha$ ) from most nuclei. This is

$$\begin{aligned} U_{opt}(r) = & V_C(r) && \text{a Coulomb term,} \\ & -Vf_V(r) - iWf_W(r) && \text{volume terms,} \\ & +V_Sg_V(r) - iW_Sg_W(r) && \text{surface terms,} \\ & -d_{so}\vec{l} \cdot \vec{s}(V_{so}h_V(r) - iW_{so}h_W(r)), && \text{spin-orbit terms} \end{aligned}$$

where the spin-orbit constant is  $d_{so} = (\hbar/m_\pi c)^2 \approx 2 \text{ fm}^2$ .

The Coulomb potential is usually taken to be the interaction of a point charge with a uniformly-charged sphere of radius  $R_c = 1.25 * A^{1/3}$  (fm),

$$V_C(r) = \begin{cases} \frac{Z_p Z_T e^2}{2R_c} \left( 3 - (r/R_c)^2 \right) & r < R_c \\ \frac{Z_p Z_T e^2}{r} & r > R_c \end{cases}$$

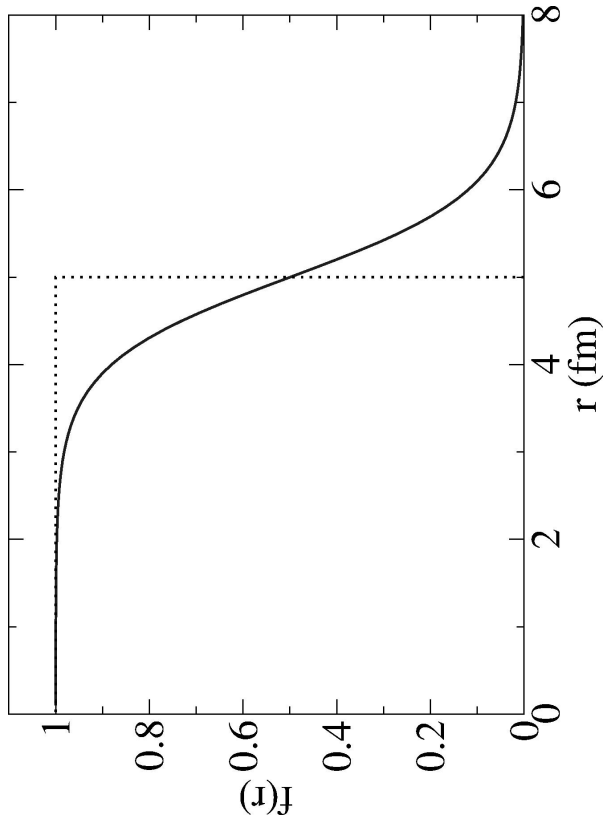
# The volume terms of the optical potential

The volume terms are usually taken to be of Wood-Saxon form,

$$f_i(r) = \frac{1}{1 + \exp[(r - R_i)/a_i]} \quad i = V, W,$$

where  $R_i$  and  $a_i$  are the radii and diffusivities of the two terms.

The Wood-Saxon form is quite similar to the nucleon density of a saturated nucleus ( $A > 30$ ).



The real volume potential reflects the average interaction of the projectile with the nucleons of the target. The strength of the real volume potential is roughly proportional to the mass of the projectile and decreases with energy, in agreement with nuclear mean field calculations.

The imaginary volume potential takes into account the loss of projectile flux due to collisions with the nucleons in the target. It is zero at low energy, below the threshold for single-particle excitations, and increases with energy as the phase space of single-particle modes increases.

# The surface terms of the optical potential

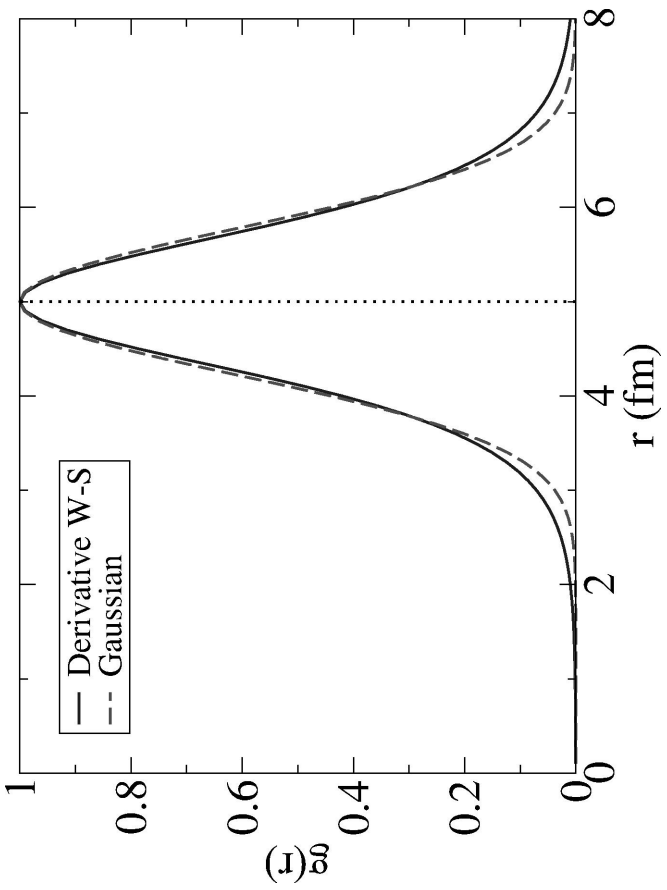
The surface terms are usually taken to be either the derivative of a Woods-Saxon,

$$g_i(r) = -4a_i \frac{d}{dr} f_i(r) = 4 \frac{\exp[(r-R_i)/a_i]}{\left(1+\exp[(r-R_i)/a_i]\right)^2} \quad i = V, W,$$

or a Gaussian,

$$g_i(r) = \exp\left[\left(r-R_i\right)^2/a_i^2\right] \quad i = V, W.$$

The two are practically indistinguishable when  $a_G=2.21 a_{WS}$ .



The imaginary surface term takes into account the absorption due to the excitation of low-energy collective modes, which have their couplings concentrated on the surface.

A real surface term can result from the same coupling but can also be explained using a dispersion relation.

## The spin-orbit terms of the optical potential

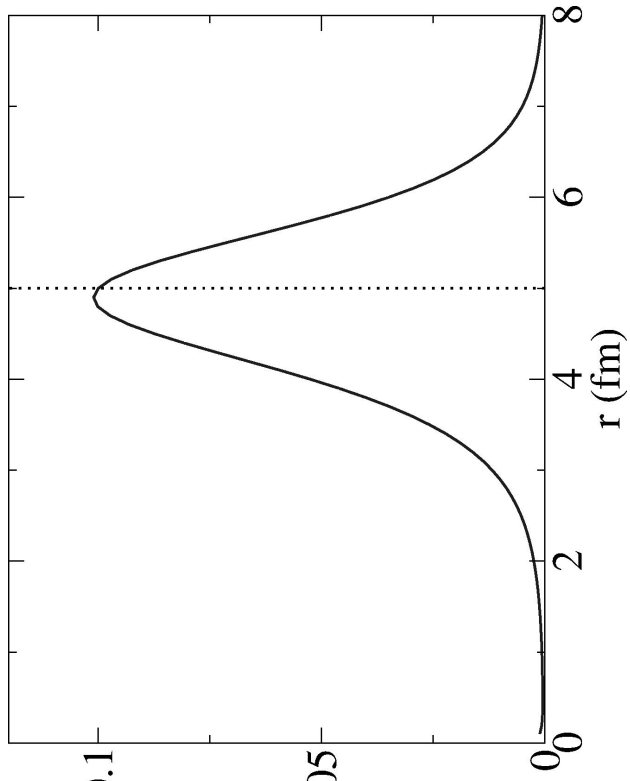
The spin-orbit terms are taken to have a Thomas form factor,

$$h_i(r) = -\frac{1}{r} \frac{d}{dr} f_i(r) = \frac{1}{ra_i} \frac{\exp[(r-R_i)/a_i]}{r a_i \left(1 + \exp[(r-R_i)/a_i]\right)^2} \quad i = V, W.$$

The spin-orbit interaction also acts between the bound states of a nucleus, where it increases the binding of the  $j=l+\frac{1}{2}$  levels and decreases the binding of the  $j=l-\frac{1}{2}$  levels.

The Thomas form factor and the spin-orbit potential itself are obtained (for spin  $\frac{1}{2}$ ) when the Dirac equation with Wood-Saxon potentials is reduced to an equivalent Schrödinger equation.

The spin-orbit interaction is thus another manifestation of the volume interaction of the projectile with the nucleons of the target.



# Optical potential parameters

The phenomenological optical potential is thus parametrized in terms of a set of potential strengths and corresponding geometrical parameters.

The best modern reference for optical potential parameters is the Reference Input Parameter Library (RIPL), available both online and in CD from the International Atomic Energy Agency.

For nucleons, typical values of the potential strengths are

$$\begin{aligned} V &\approx (45 - 55) \text{ MeV} - (0.2 - 0.3)E, \\ W_s &\approx (2 - 7) \text{ MeV} - (0.1 - 0.3)E \quad E < 8 - 10 \text{ MeV}, \\ V_{so} &\approx (4 - 10) \text{ MeV}. \end{aligned}$$

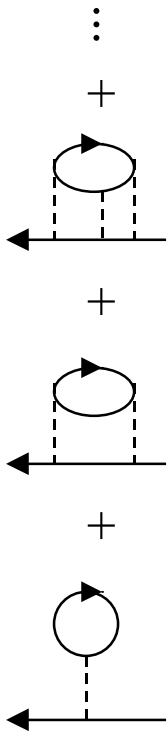
Above 8-10 MeV,  $W_s$  is usually constant or slightly decreasing.  $V_s$  and  $W_{so}$  can normally be taken to be zero as can  $W$  below about 10 MeV. Above about 10 MeV,  $W$  is constant or slightly increasing.

The radii  $R_i$  take on values  $R_i = r_i A_T^{1/3}$  with the reduced radii in the range  $r_i \approx 1.2 - 1.3$  fm. The diffusivities are normally in the range  $a_i \approx 0.4 - 0.7$  fm.

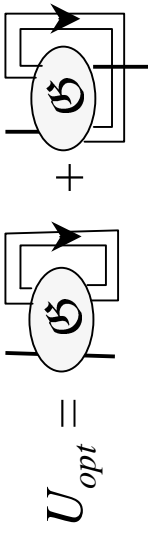
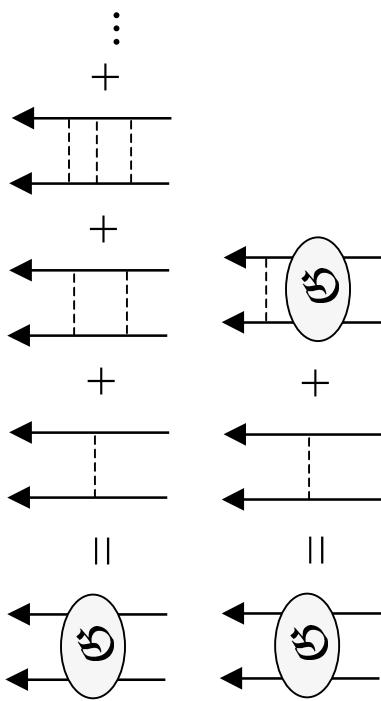
Fairly wide ranges of the parameters  $V$ ,  $R_V$ ,  $W_s$  and  $a_s$  result in equally good fits if  $VR_V^2$  and  $W_s a_s$  remain constant. These are potential ambiguities.

# The microscopic optical potential -- I

Microscopic optical potentials attempt to describe the projectile-target interaction in terms of nucleon-nucleon interactions, such as these representing the first few terms in nucleon-nucleus interaction.



A systematic method for summing the most important terms is provided by the self-consistent Brueckner approximation. The Brueckner  $\mathcal{G}$ -matrix is calculated by summing repeated interactions, taking into account effects of the nuclear medium. This calculation is usually performed in infinite nuclear matter, for simplicity.



The  $\mathcal{G}$ -matrix is then folded over the target nucleon density to obtain the optical potential  $U$ . Self-consistency requires that the target density be obtained with the same potential.

$$U_{opt} = \boxed{\mathcal{G}} + \boxed{\mathcal{G}}$$

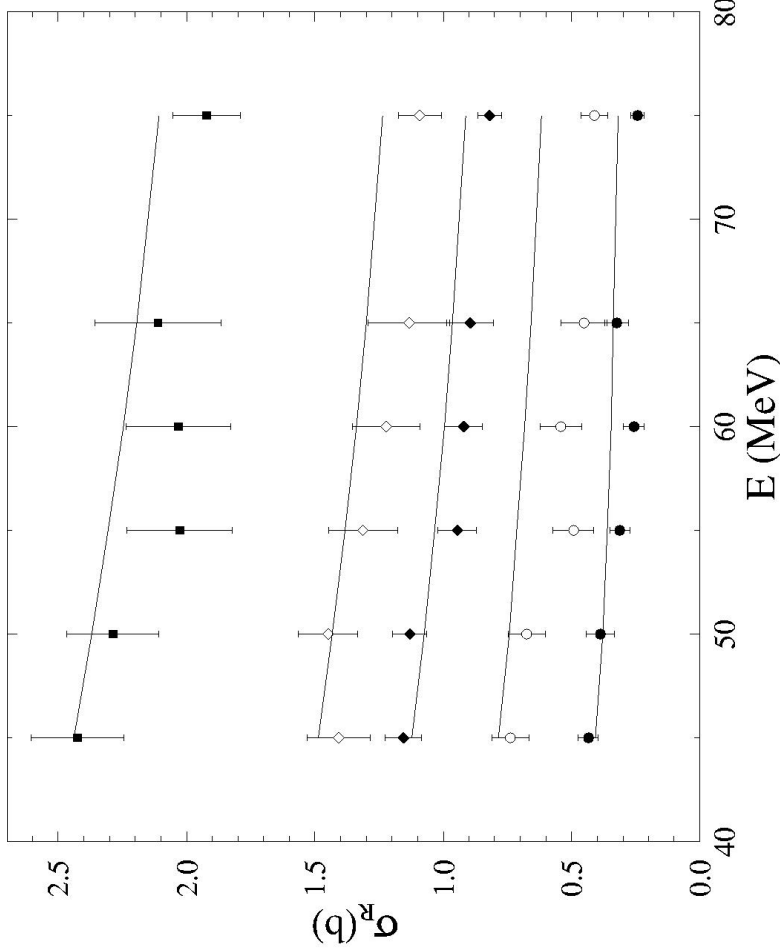
## The microscopic optical potential -- II

The microscopic optical potential possesses a direct term and an exchange term. The exchange term is non-local and both are energy-dependent. The exchange term is often approximated as a local term with an additional energy-dependence (JLM).

At high energy, the microscopic optical potential reduces to the impulse approximation potential, obtained by folding the two-nucleon  $t$ -matrix with the target density -- the  $t\rho$  approximation.

The figure compares experimental reaction cross sections for  $^{12}\text{C}$ ,  $^{28}\text{Si}$ ,  $^{56}\text{Fe}$ ,  $^{90}\text{Zr}$  and  $^{208}\text{Pb}$ , in ascending order, with microscopic optical model calculations by Amos and Karataglidis, nucl-th/0202050.

$$U_{opt} = \boxed{\text{G}} + \boxed{\text{G}} + U_d + U_{ex}$$



# The microscopic potential at low energy

Formally, we derived the optical potential by considering the scattering in a subspace  $\mathcal{P}$  of the space of states and then energy-averaged to smooth the dependence on the remaining subspace of states  $\mathcal{Q}$ . We obtained

$$U_{opt} = V_{PP} + V_{PQ} \frac{1}{E - H_{QQ} + i\Delta/2} V_{QP}.$$

In the microscopic optical potential, the division into  $\mathcal{P}$  and  $\mathcal{Q}$  subspaces is no longer transparent. It is there, contained in the  $\mathcal{G}$ -matrix, but in terms of nucleon-nucleon scattering rather than nucleon-nucleus scattering. We would thus expect that the microscopic potential does not take into account the collective effects that are often important at low energies. We might consider decomposing the optical potential at low energies (using a local approximation) as

$$U_{opt}(r, E) = U_{sp}(r, E) + U_{coll}(r, E),$$

where  $U_{sp}$  is the microscopic potential and  $U_{coll}$  is the remainder, which we might attribute to collective effects. At low energies,  $U_{sp}(r, E) \approx V_{HF}(r, E)$ . At high energy, we expect that  $U_{coll}(r, E) \rightarrow 0$ .

## Dispersion relations

Because of causality, the optical potential should have no singularities in the upper half-energy plane. We may then write

$$\oint dE' \frac{U_{coll}(r, E')}{E' - E} = 0,$$

which we may rewrite as

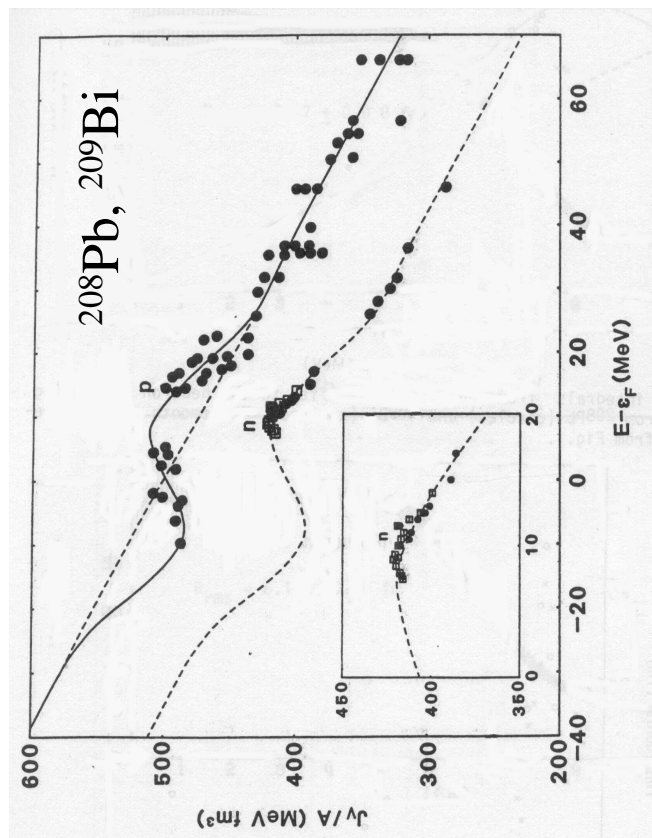
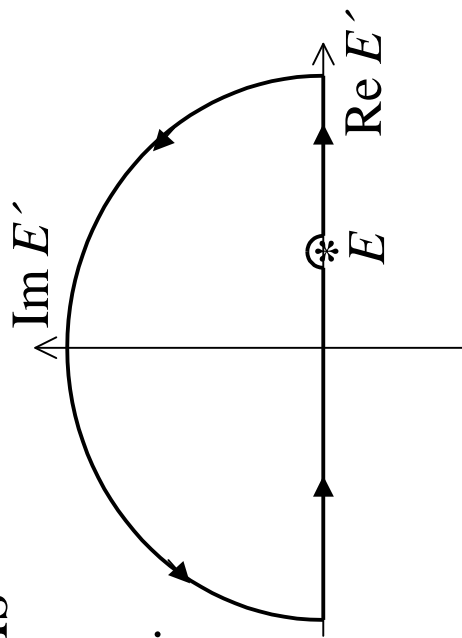
$$\text{P.P.} \int dE' \frac{U_{coll}(r, E')}{E' - E} = i\pi U_{coll}(r, E)$$

Separating  $U_{coll}$  into its real and imaginary parts,  $U_{coll} = \Delta V + i W$ , we have

$$\Delta V(r, E) = \text{P.P.} \frac{1}{\pi} \int dE' \frac{W(r, E')}{E' - E}$$

At low energy,  $U_{opt} \approx V_{HF} + \Delta V + i W$ .

The effect of  $\Delta V$  is seen as a strengthening in the real part of the optical potential at low energy relative to the linear dependence expected of  $V_{HF}$ .



(Finlay and Petler, Opt. Model 1986)

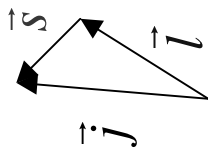
# The single-channel optical model -- spin

Because of the spin-orbit interaction, a rigorous treatment of neutron or proton scattering requires that the spin be included in the calculation. To do this, one performs the partial wave expansion of the scattering wave function (spin  $s$ ) as

$$\Psi = \frac{4\pi}{kr} \sum_{ljn} i^l e^{i\sigma_l} \psi_l^j(r) \mathfrak{Y}_{ls}^{jn}(\hat{r}) \mathfrak{Y}_{ls}^{jn\dagger}(\hat{k}),$$

in terms of the spin-angular functions,

$$\mathfrak{Y}_{ls}^{jn}(\hat{r}) = i^l \sum_{mv} \langle lmsv | jn \rangle Y_{lm}(\hat{r}) | sv \rangle,$$



where  $l$  and  $j$  are the orbital and total angular momenta and  $|sv\rangle$  is a spin eigenvector. In the expansion,  $\sigma_l$  is the Coulomb phase shift,  $\hat{r}$  denotes the angular variables and  $\hat{k}$  the direction of the incident momentum. The spin-angular functions are vectors with components labeled by  $v$ , the projection of the spin.

Because of angular momentum and parity conservation, the equations for the  $\psi_l^j(r)$  uncouple. They can then be solved as before and the asymptotic behavior of the resulting wave function analyzed to extract the scattering amplitude.

# The scattering amplitude -- spin

The scattering amplitude

$$f(\theta) = f_c(\theta) \mathbf{1} + \frac{4\pi}{2ik} \sum_{jn} e^{2i\sigma_l} (S_i^j - 1) \mathfrak{D}_{ls}^{jn}(\hat{r}) \mathfrak{D}_{ls}^{jn\dagger}(\hat{k}),$$

with  $f_c(\theta)$  the Coulomb scattering amplitude, is now a matrix,  $\mathbf{f}_{\nu\nu'}(\theta)$ , with matrix elements labeled by the spin projections  $\nu$  and  $\nu'$ .

For particles of spin  $1/2$ ,

$$\mathbf{f}(\theta) = \begin{pmatrix} A(\theta) & B(\theta) \\ B(\theta) & A(\theta) \end{pmatrix}$$

where

$$A(\theta) = f_c(\theta) + \frac{1}{2ik} \sum_l e^{2i\sigma_l} \left[ (l+1)(S_l^{l+1/2} - 1) + l(S_l^{l-1/2} - 1) \right] P_l(\cos\theta),$$

$$\text{and } B(\theta) = \frac{1}{2ik} \sum_l e^{2i\sigma_l} \left[ S_l^{l+1/2} - S_l^{l-1/2} \right] P_l^1(\cos\theta).$$

The amplitude  $A$  corresponds to scattering in which the spin projection remains constant. The amplitude  $B$  describes scattering in which the spin projection flips.



## Angular distributions -- spin

The differential elastic cross section for an unpolarized incident beam is obtained by averaging the squared magnitudes of the scattering amplitudes over the initial values of the projectile spin and summing over the final ones,

$$\frac{d\sigma}{d\Omega} = \frac{1}{2s+1} \sum_{\nu\nu'} |f_{\nu\nu'}(\theta)|^2.$$

For spin-1/2 particles, this becomes

$$\frac{d\sigma}{d\Omega} = |A(\theta)|^2 + |B(\theta)|^2 \quad s = 1/2.$$

For particles of spin 1/2 and greater, vector and possibly tensor spin observables may be defined in terms of other combinations of the amplitudes. For particles of spin 1/2, the vector polarization  $P(\theta)$  and the spin rotation function  $Q(\theta)$  are defined as

$$P(\theta) = \frac{2 \operatorname{Im} A^*(\theta)B(\theta)}{d\sigma/d\Omega} \quad \text{and} \quad Q(\theta) = \frac{2 \operatorname{Re} A^*(\theta)B(\theta)}{d\sigma/d\Omega}.$$

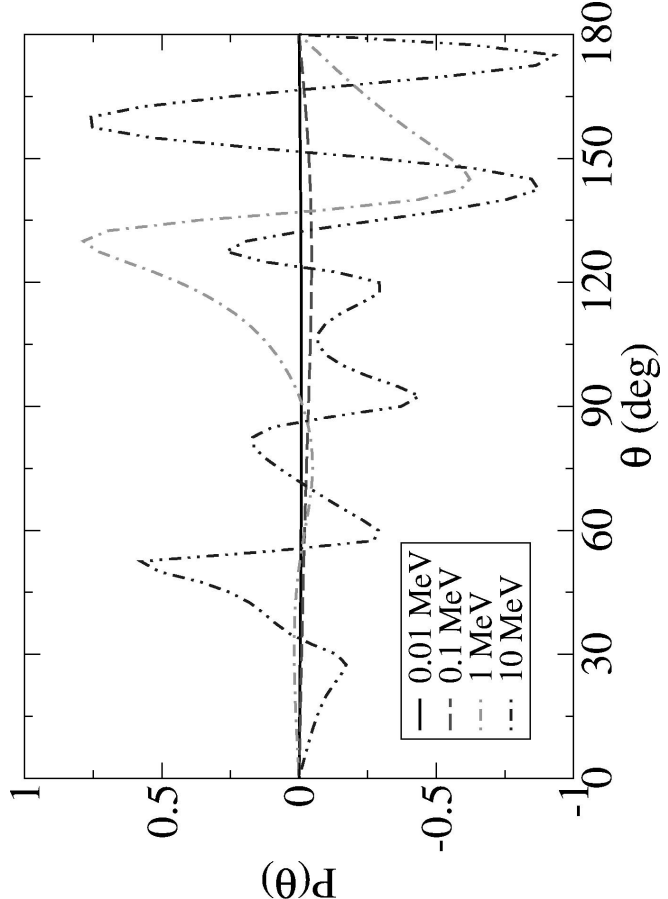
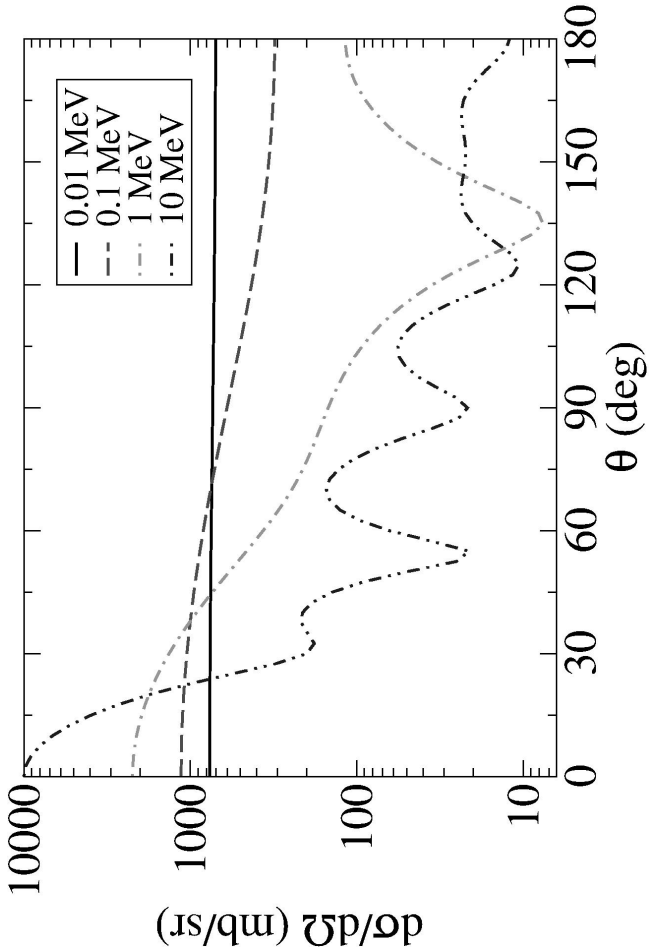
## Polarization in neutron scattering

The spin-summed angular distribution due to scattering of a polarized beam may be written as

$$\frac{d\sigma_{pol}}{d\Omega} = \frac{d\sigma}{d\Omega} \left( 1 + P(\theta) \hat{n} \cdot \vec{P}_{pol} \right),$$

where  $\vec{P}_{pol}$  is a vector defining the initial polarization and  $\hat{n}$  is the normal to the scattering plane.

The spin-orbit interaction is fairly strong. Its effects on the polarization become visible as soon as partial waves above the s-wave contribute to the scattering.



## Integrated cross sections -- spin

As before, the absorption cross section may be related to flux lost from the asymptotic probability current density,

$$\sigma_{abs} = -\frac{1}{v} \oint_S \vec{j} \cdot d\vec{S} = \frac{1}{2s+1} \frac{\pi}{k^2} \sum_{lj} (2j+1) \left( 1 - |S_l^j|^2 \right).$$

The fraction of the flux lost from each partial wave may also be expressed as a transmission coefficient,

$$T_l^j = 1 - |S_l^j|^2.$$

For charged particles, the Coulomb interaction leads to an infinite elastic cross section. For neutrons, integration of the differential cross section yields

$$\sigma_{el} = \int d\Omega \frac{d\sigma}{d\Omega} = \frac{\pi}{2k^2} \sum_{lj} (2j+1) |S_l^j - 1|^2.$$

For neutron, the total cross section may be defined as the sum of the elastic and absorption ones,

$$\sigma_{tot} = \sigma_{el} + \sigma_{abs} = \frac{\pi}{k^2} \sum_{lj}^{\infty} (2j+1) \left( 1 - \text{Re } S_l^j \right).$$

## Comparison with experiment

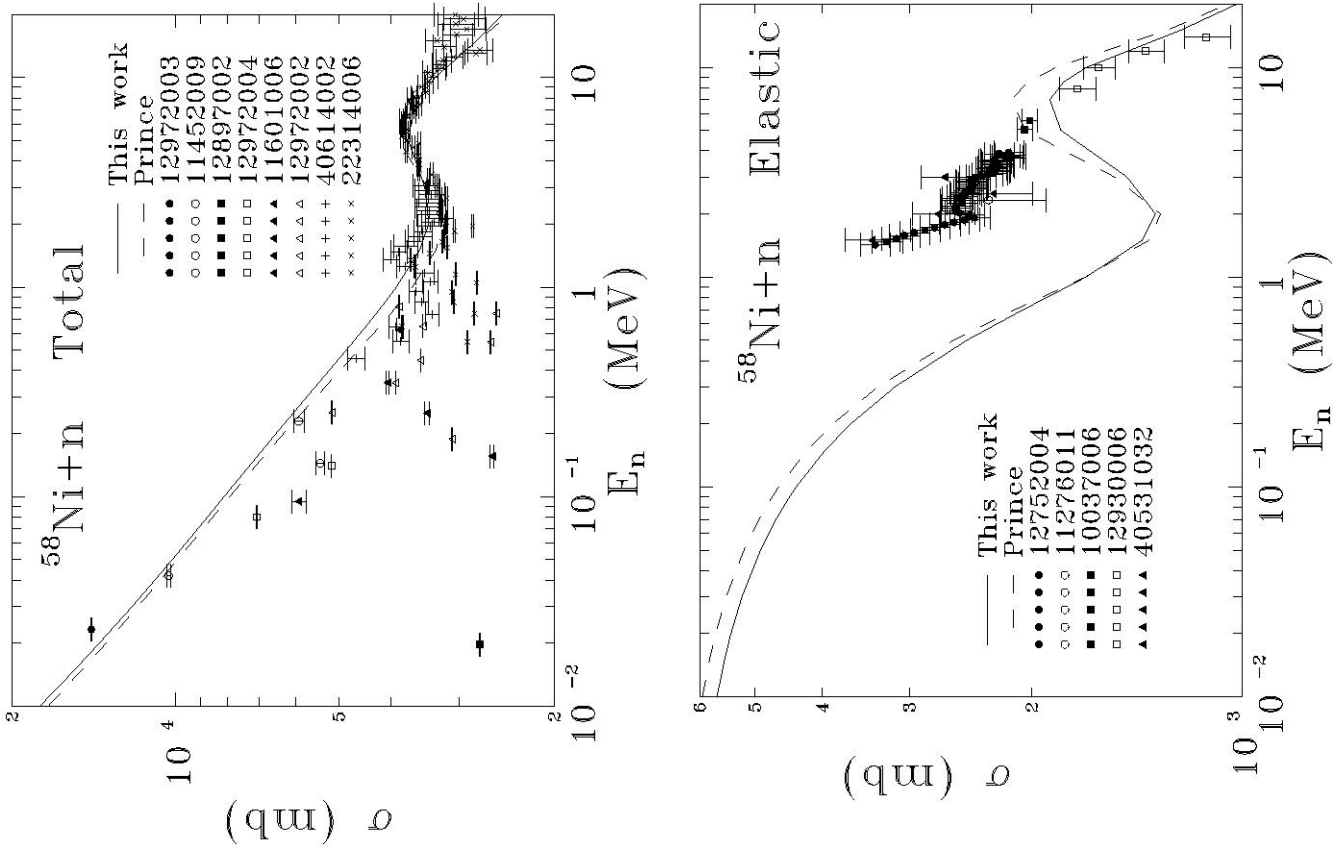
We recall that, being linear in the scattering amplitude, the total optical cross section may be compared to the energy-averaged experimental one. We see that reasonable agreement with the data is possible here.

We also verified that the partial wave contributions to the energy-averaged elastic cross section,

$$\sigma_{l,el}^j = \frac{\pi}{k^2} |S_l^j - 1|^2 + \frac{\pi}{k^2} \left\langle \left| S_{l,fluc}^j \right|^2 \right\rangle$$

exceed the shape elastic (optical) ones due to contributions from fluctuations.

We observe that the fluctuation contributions are negligible only at higher energies.



## Inelastic scattering

The single-channel optical model describes the scattering in the elastic channel alone. It is often called the spherical optical model because, in it, the target may be considered to be spherically symmetric since its structure is never introduced.

Direct reactions that transfer energy as well as momentum are often quite important. Such inelastic scatterings, in the case of the inert projectiles that we are considering ( $n$ ,  $p$ ,  $\alpha$ ,  $d$ , etc.), leave the target in an excited state and diminish the asymptotic kinetic energy of the projectile. To describe inelastic scattering, we must introduce at least the basic characteristics of the ground and excites states of the target.

The nature of the ground and excited states of the target nucleus are also important factors in determining the degree to which the target is excited in a collision. The states that are most strongly excited in collisions are those that involve collective movement, vibrations and rotations, in particular.

# Vibrations

Every nucleus possesses collective vibrational modes of excitation. Their importance in low-energy scattering, however, varies greatly from nucleus to nucleus.

Vibrational modes may be understood qualitatively as shape oscillations of intermixed but incompressible neutron and proton fluids about their equilibrium configuration. The protons and neutrons may oscillate in phase (isoscalar) or out of phase (isovector) with one another.

The simplest modes are:

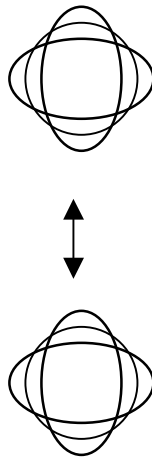
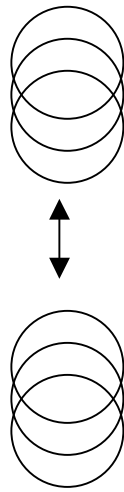
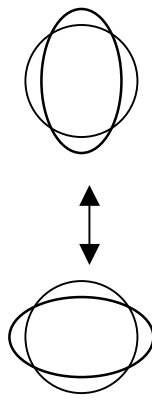
Isoscalar

$l=1^-$  – dipole

CM displacement

Isovector

$l=2^+$  -- quadrupole



Octupole ( $l=3^-$ ) modes are also common and many others have been observed.

# Vibrations – Excitation Energies and states

Isovector vibrations occur at higher energies than the corresponding isoscalar ones, because of the strong nuclear attraction between protons and neutrons.

Negative parity vibrational modes tend to vary smoothly in energy as a function of the mass number. Positive parity vibrational modes, vary greatly with the mass and depend on the shell structure. The variations in the excitation energies are explained in a microscopic treatment in terms of particle-hole pairs:

Negative parity – particle-hole pairs from two adjacent shells,

Positive parity – particle-hole pairs from same shell, when possible,  
otherwise from one shell and from second higher shell.

Ex.:  $^{208}\text{Pb}$  – the first excited state is the 3- octupole state.

Vibrations are bosonic modes. Multiple excitations are possible but must form symmetric states. Thus an excited state consisting of two  $l=2^+$  quadrupole phonons on a  $I=0^+$  ground state may have  $I=0^+, 2^+, 4^+$ .

The states may be written in terms of creation operators  $b_{I_c N_c}^\dagger$  as

$$|cI_c N_c\rangle = b_{I_c N_c}^\dagger |0\rangle \quad \text{and} \quad |c_1 c_2 I_c N_c\rangle = \frac{1}{\sqrt{1+\delta_{I_1 I_2}}} [b_{I_1}^\dagger b_{I_2}^\dagger]_{I_c N_c} |0\rangle$$

# Vibrations – An example

In the simplest case of non-interacting phonons, the spectrum is harmonic. The ideal spectrum of the first few excited quadrupole states on an I=0<sup>+</sup> ground state are shown here.

We compare this with the first few excited states of <sup>58</sup>Ni (energies in MeV).

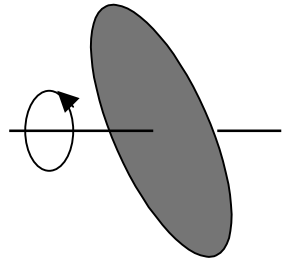
$$\begin{array}{lll} E_x = 2\hbar\omega & \text{---} & I=0^+, 2^+, 4^+ \\ E_x = \hbar\omega & \text{---} & I=2^+ \\ E_x = 0 & \text{---} & I=0^+ \\ & \text{Ideal} & \end{array}$$

$$\begin{array}{lll} E_x = 2.46, 2.78, 2.90, 2.94 & \text{---} & I=4^+, 2^+, 1^+, 0^+ \\ E_x = 1.45 & \text{---} & I=2^+ \\ E_x = 0 & \text{---} & I=0^+ \\ & ^{58}\text{Ni} & \end{array}$$

The three states that can be interpreted as two-phonon quadrupole states occur close in energy to twice the energy of the one-phonon state and have the correct spin and parity. The 1<sup>+</sup> state, however, does not.

Another indicator of the relationship between the states are the branching ratios for their EM decay. The two-phonon 4<sup>+</sup> and 2<sup>+</sup> states decay almost exclusively to the one-phonon 2<sup>+</sup> state, as does the 1<sup>+</sup> state. The two-phonon 0<sup>+</sup> state decays to various of the others, but principally to the 1<sup>+</sup> state.

## Rotations



Many nuclei in the regions between closed shells possess a statically deformed ground state with axial symmetry. The lowest energy excited states of these nuclei are usually rotations about an axis perpendicular to the symmetry axis.

We can approximate the surface of a deformed nucleus as

$$R(\theta') = R_0 \left( 1 + \sum_{\lambda} \beta_{\lambda} Y_{\lambda 0}(\theta') \right),$$

where the  $\beta_{\lambda}$ ,  $\lambda=2, 4, 6, \dots$  are deformation parameters and the angle  $\theta'$  is taken with respect to the symmetry axis of the nucleus. The most important of the deformation parameters is  $\beta_2$ .

When  $\beta_2 < 0$ , the nucleus is oblate. When  $\beta_2 > 0$ , the nucleus is prolate.

The wave function of a rotational state can be written in terms of an intrinsic wave function  $\chi_K$  and the rotation matrices  $D_{NK}^I$  as

$$\langle \vec{r}_{\text{int}} | c I_c N_c \rangle = \frac{1}{\sqrt{1 + \delta_{K0}}} \sqrt{\frac{2I_c + 1}{16\pi^2}} \left[ \chi_K(\vec{r}_{\text{int}}) D_{N_c K}^{I_c *}(\hat{r}_{\text{int}}) + (-)^{I_c - I_x} \chi_{-K}(\vec{r}_{\text{int}}) D_{N_c - K}^{I_c *}(\hat{r}_{\text{int}}) \right]$$

where  $K$  is the projection of the intrinsic ang. momentum  $\chi$  on the symmetry axis.

## Rotations – An example

A rotational band built on a  $0^+$  ground state consists of states with  $I=0^+, 2^+, 4^+, 6^+, \dots$ . A rotational band built on a ground state with spin  $I_0 \neq 0$  consists of states with  $J=I_0, I_0+1, I_0+2, I_0+3, \dots$

The excitation energy of a state with angular momentum  $I$  is

$$E_x(I) = \frac{\hbar^2}{2J} [I(I+1) - I_0(I_0 + 1)].$$

The nucleus  $^{238}\text{U}$  possesses static deformations of  $\beta_2=0.198$  and  $\beta_4=0.057$ . The rotational band based on its  $0^+$  ground state consists of excited states with

$$\begin{aligned} I=2^+ & E_x=0.045 \text{ MeV} = 0.0075 \text{ MeV} * 2^*3, \\ I=4^+ & E_x=0.148 \text{ MeV} = 0.0074 \text{ MeV} * 4^*5, \\ I=6^+ & E_x=0.307 \text{ MeV} = 0.0073 \text{ MeV} * 6^*7, \\ I=8^+ & E_x=0.518 \text{ MeV} = 0.0072 \text{ MeV} * 8^*9, \\ & \vdots \\ I=28^+ & E_x=4.516 \text{ MeV} = 0.0056 \text{ MeV} * 28^*29, \text{ and possibly more.} \end{aligned}$$

The electromagnetic decay of each of these states occurs exclusively to the next state of lower energy in the chain.

## The generalized optical potential – vibrations

The simplest manner of extending the optical potential to take into account either static deformation or the dynamical deformation of a vibrational mode is to modify the radii of the terms in the potential accordingly.

In its simplest form, a vibrational mode of a nucleus may be taken as a shape oscillation about a spherical equilibrium mode. The radii of the terms in the potential may be expressed as

$$R_i = R_{0i} \left( 1 + \sum_{\lambda\mu} a_{\lambda\mu} Y_{\lambda\mu}(\hat{r}) \right), \quad \text{with} \quad a_{\lambda\mu} = \frac{\beta_\lambda}{\sqrt{2\lambda+1}} (b_{\lambda\mu}^\dagger + (-)^\mu b_{\lambda-\mu}),$$

where  $b_{\lambda\mu}^\dagger$  and  $b_{\lambda\mu}$  are the phonon creation/annihilation operators and the  $\beta_\lambda$  are the amplitudes of the shape oscillations.

We may then expand the optical potential in the creation/annihilation operators as

$$U_{opt}(\vec{r}) = U_{opt}(r) + \sum_i \frac{\partial U_{opt}}{\partial R_i} R_{0i} \sum_{\lambda\mu} a_{\lambda\mu} Y_{\lambda\mu}(\hat{r}).$$

The potential is sometimes expanded to second order in the operators. The second order potential permits single-step transitions to two-phonon states.

## The generalized optical potential -- rotations

The optical potential for a deformed nucleus may also be obtained by expanding the deformed potential radii

$$R_i(\theta') = R_{0i} \left( 1 + \sum_{\lambda} \beta_{\lambda} Y_{\lambda 0}(\theta') \right),$$

in a Taylor series in the deformation parameters,  $\beta_{\lambda}$ . However, when the deformations are large, it is better to expand it directly in multipoles as

$$U_{opt}(r, \hat{r}') = \sum_{\lambda} U_{\lambda}(r) Y_{\lambda 0}(\hat{r}') \quad \text{with} \quad U_{\lambda}(r) = \int d\Omega' U_{opt}(r, \theta') Y_{\lambda 0}(\theta').$$

The moments  $U_{\lambda\mu}(r)$ , with  $\mu \neq 0$ , vanish in the body-fixed frame. The body-fixed angles  $\hat{r}'$  are related to the space fixed ones  $\hat{r}$  through the collective angular coordinates of the nucleus,  $\hat{r}_{int}$ . This implies that

$$Y_{\lambda 0}(\hat{r}') = \sum_{\mu} Y_{\lambda\mu}(\hat{r}) D_{\mu 0}^{\lambda}(\hat{r}_{int}) = \sum_{\mu} Y_{\lambda\mu}(\hat{r}) Y_{\lambda\mu}^{*}(\hat{r}_{int}).$$

The optical potential in the rotational model may thus be expanded as

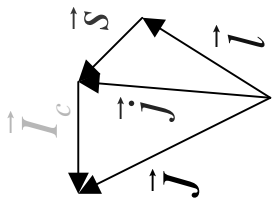
$$U_{opt}(\vec{r}, \hat{r}_{int}) = \sum_{\lambda\mu} U_{\lambda}(r) Y_{\lambda\mu}(\hat{r}) Y_{\lambda\mu}^{*}(\hat{r}_{int}).$$

The generalized optical potential, in both models, couples the relative motion to the internal degrees of freedom of the target.

# Coupled-channels partial wave expansion

To properly take into account the angular momentum of the target, the spin-angular functions must be coupled to the target states to form target-spin-angular functions of total angular momentum  $J$  and projection  $M$ ,

$$\mathfrak{D}_{lsjc}^{JM}(\hat{r}) = \sum_{nN_c} \left\langle jnl_c N_c | JM \right\rangle \mathfrak{D}_{ls}^{jn}(\hat{r}) \left| cI_c N_c \right\rangle.$$



The functions also depend on the internal target coordinates. In terms of these, the scattering wave function may be expanded in a sum over both the excited states and angular momenta,

$$\Psi = 4\pi \sum_{\substack{l'j'c \\ l'j'c'}} \mathfrak{D}_{l'sj'c'}^{JM}(\hat{r}) i^{l'} \psi_{l'j'c'ljc}^J(r) \frac{e^{i\sigma_{lc}}}{k_c r} \mathfrak{D}_{lsjc}^{JM\dagger}(\hat{k}).$$

The most significant difference here is that the partial wave functions depend on two sets of indices,  $l$ ,  $j$ ,  $c$  and  $l'$ ,  $j'$ ,  $c'$ . For a particle with spin in the spherical optical model, we have two indices  $l$  and  $l'$ , in principal, for each value of the total angular momentum  $j$ . For particles of spin 0 or spin  $1/2$ , parity conservation reduces the two,  $l$  and  $l'$ , to have the same value. The partial wave functions and S-matrix elements are then uncoupled scalar quantities. Here, we should look more carefully to see how the channels could be coupled.

# Coupled partial waves

To analyze the partial waves that can couple, we must consider all possible combinations of the orbital angular momentum  $l$ , the spin  $s$ , the channel angular momentum  $j$  and the target spins  $I_c$  that can sum to a given value  $J$  of the total angular momentum and possess a given value of the parity,  $\pi$ .

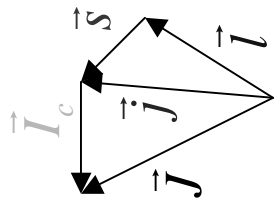
Consider a simple example: a spin- $1/2$  nucleon incident on a  $0^+$  ground state that can be excited to a  $2^+$  target state. We have

For the  $J^\pi=1/2^+$  channel:

- |                                |          |                                |
|--------------------------------|----------|--------------------------------|
| 0+ ground state: $l=0, j=1/2$  | 3        | 0+ ground state: $l=1, j=1/2$  |
| 2+ excited state: $l=2, j=3/2$ | coupled  | 2+ excited state: $l=1, j=3/2$ |
| $l=2, j=5/2$                   | channels | $l=3, j=5/2$                   |

For the  $J^\pi=5/2^+$  channel:

- |                                |          |                                |
|--------------------------------|----------|--------------------------------|
| 0+ ground state: $l=2, j=5/2$  | 6        | 0+ ground state: $l=3, j=5/2$  |
| 2+ excited state: $l=0, j=1/2$ | coupled  | 2+ excited state: $l=1, j=1/2$ |
| $l=2, j=3/2$                   | channels | $l=1, j=3/2$                   |
| $l=2, j=5/2$                   |          | $l=3, j=5/2$                   |
| $l=4, j=7/2$                   |          | $l=3, j=7/2$                   |
| $l=4, j=9/2$                   |          | $l=5, j=9/2$                   |



For the  $J^\pi=1/2^-$  channel:

- |                               |   |                               |
|-------------------------------|---|-------------------------------|
| 0+ ground state: $l=1, j=1/2$ | 6 | 0+ ground state: $l=1, j=1/2$ |
| $l=3, j=5/2$                  |   | $l=3, j=5/2$                  |

For the  $J^\pi=5/2^-$  channel:

- |                               |   |                               |
|-------------------------------|---|-------------------------------|
| 0+ ground state: $l=3, j=5/2$ | 6 | 0+ ground state: $l=3, j=5/2$ |
| $l=1, j=1/2$                  |   | $l=1, j=1/2$                  |
| $l=3, j=5/2$                  |   | $l=3, j=5/2$                  |
| $l=5, j=7/2$                  |   | $l=5, j=7/2$                  |
| $l=5, j=9/2$                  |   | $l=5, j=9/2$                  |

# The coupled equations

When the partial-wave expansion is substituted in the Schrödinger equation, it reduces to a set of coupled equations for each value of  $J^\pi$ ,

$$\frac{\hbar^2}{2\mu} \left\{ \frac{d^2}{dr^2} - \frac{l(l'+1)}{r^2} + k_c^2 \right\} \Psi_{l'j'c',ljc}^J(r) - \sum_{l''j''c''} \mathfrak{U}_{l'j'c',l''j''c''}^J(r) \Psi_{l''j''c'',ljc}^J(r) = 0,$$

where the potential matrix elements are those of the target-spin-angular functions,  $\mathfrak{U}_{l'j'c',ljc}^J(r) = \int d\Omega \mathfrak{D}_{l'sj'c'}^{JM\dagger}(\hat{r}) U_{opt}(\vec{r}, \vec{r}_{\text{int}}) \mathfrak{D}_{lsjc}^{JM}(\hat{r})$ .

The matrix elements are independent of M due to rotational invariance and symmetric under interchange of indices, if the system is time-reversal invariant.

If we group the matrix elements of the coupled equations into matrices,

$$l' \delta_{l'l} \delta_{j'j} \delta_{c'c} \rightarrow L_J \quad k_c \delta_{l'l} \delta_{j'j} \delta_{c'c} \rightarrow K_J \\ \Psi_{l'j'c',ljc}^J(r) \rightarrow \Psi_J(r) \quad \mathfrak{U}_{l'j'c',ljc}^J(r) \rightarrow U_J(r)$$

We may write the coupled equations for each value of  $J^\pi$  as a matrix equation

$$\left\{ \frac{d^2}{dr^2} - \frac{L_J(L_J+1)}{r^2} + K_J^2 - \frac{2\mu}{\hbar^2} U_J(r) \right\} \Psi_J(r) = 0.$$

# The scattering amplitude and S-matrix

We may also introduce the target-spin angular functions into the matrix representation of the partial wave decomposition, but as a vector rather than as a matrix,

$$\mathfrak{D}_{lsjc}^{JM}(\hat{r}) = \langle \hat{r} | lsjcJM \rangle \rightarrow \langle \hat{r} | JM \rangle.$$

The wave function may then be written as

$$\Psi = \frac{4\pi}{r} \sum_{JM} \langle \hat{r} | JM \rangle i^{L_J} \Psi_J(r) e^{i\sigma_J} K_J^{-1} \langle JM | \hat{k} \rangle.$$

Conceptually, obtaining the scattering amplitude is now straightforward. As before, the wave function must be integrated numerically from the origin to beyond the range of the nuclear potential. There, it is matched to either Coulomb or free waves (in matrix form),

$$\Psi_J \rightarrow \frac{i}{2} (H_J^-(r) - H_J^+(r) e^{i\sigma_J} \bar{S}_J e^{i\sigma_J}) e^{-i\sigma_J} \quad \text{where} \quad \bar{S}_{l'j'c'jfc}^J \rightarrow \bar{S}_J.$$

Substituting this expression in the partial wave expansion and analyzing its asymptotic form, we obtain the scattering amplitude,

$$\bar{f}(\theta) = \frac{4\pi}{2i} \sum_{JM} \langle \hat{r} | JM \rangle (e^{i\sigma_J} \bar{S}_J e^{i\sigma_J} - 1_J) K_J^{-1} \langle JM | \hat{k} \rangle.$$

The matrix elements of the scattering amplitude,  $\bar{f}_{v'N_c c' v N_c c}$ , are labeled by the target state and the projections of the projectile and target spins.

## Flux normalization

The cross section can be defined in terms of a ratio of current densities or fluxes. When energy is removed from the relative motion, as in inelastic scattering, the relative velocity and the corresponding flux are reduced. To correct for this, we must multiply the scattering amplitude by a factor of

$$\sqrt{v_f/v_i} = \sqrt{k_f/k_i}.$$

We may do this by defining first the normalized S-matrix,

$$S_J = K_J^{1/2} \bar{S}_J K_J^{-1/2},$$

and then defining the normalized scattering amplitude in its terms as

$$\begin{aligned} f(\theta) &= \frac{4\pi}{2i} \sum_{JM} \langle \hat{r} | JM \rangle \left( e^{i\sigma_J} S_J e^{i\sigma_J} - 1_J \right) K_J^{-1} \langle JM | \hat{k} \rangle \\ &= f_C(\theta) + \frac{4\pi}{2i} \sum_{JM} \langle \hat{r} | JM \rangle e^{i\sigma_J} (S_J - 1_J) e^{i\sigma_J} K_J^{-1} \langle JM | \hat{k} \rangle, \end{aligned}$$

where the Coulomb amplitude  $f_C(\theta)$  is now a matrix, diagonal in the spin projections and state indices, but different for each of the target states due to the difference in the relative motion..

## Angular distributions and cross sections

The angular distributions for an unpolarized beam and target are obtained by averaging the squared amplitude over the initial spin projections and summing over the final ones. Denoting the initial state by  $c_0$  and its spin by  $I_0$ , the differential elastic cross section is

$$\frac{d\sigma_{el}}{d\Omega} = \frac{1}{(2s+1)(2I_0+1)} \sum_{\substack{v'N_0 \\ vN_0}} \left| f_{v'N_0c_0, vN_0c_0}(\theta) \right|^2.$$

The differential inelastic cross section to an excited state  $c$  with spin  $I_c$  is

$$\frac{d\sigma_c}{d\Omega} = \frac{1}{(2s+1)(2I_0+1)} \sum_{\substack{v'N_c \\ vN_0}} \left| f_{v'N_c c, vN_0 c_0}(\theta) \right|^2.$$

For neutrons, the integrated elastic cross section is

$$\sigma_{el} = \frac{1}{2(2I_0+1)} \frac{\pi}{K_{c_0}^2} \sum_{\substack{l'j' \\ ij}} (2J+1) \left| S_{l'j'c_0, ljc_0}^J - \delta_{l'l} \delta_{j'j} \right|^2.$$

For charged or neutral particles, the inelastic cross section to an excited state  $c$  with spin  $I_c$  is

$$\sigma_c = \frac{1}{(2s+1)(2I_0+1)} \frac{\pi}{K_{c_0}^2} \sum_{\substack{l'j' \\ ij}} (2J+1) \left| S_{l'j'c, ljc_0}^J \right|^2.$$

## Absorption cross sections

Just as in the spherical optical model, we may associate an elastic absorption cross section  $\sigma_r$ , with the flux lost from the elastic channel,

$$\sigma_r = -\frac{1}{V} \oint_S \vec{j}_{c_0} \cdot d\vec{S} \quad \text{where} \quad \vec{j}_{c_0} = \frac{\hbar}{2i\mu} \left( \Psi_{c_0}^\dagger \nabla \Psi_{c_0} - (\nabla \Psi_{c_0}^\dagger) \Psi_{c_0} \right),$$

with  $\Psi_{c_0}$  being the ground-state component of the wave function. This cross section includes the flux lost to inelastic scattering as well as absorption.

We may also define a total absorption cross section  $\sigma_{abs}$  (which is smaller than the elastic one) as the flux lost from all of the channels together,

$$\sigma_{abs} = -\frac{1}{V} \oint_S \sum_c \vec{j}_c \cdot d\vec{S} \quad \text{where} \quad \vec{j}_c = \frac{\hbar}{2i\mu} \left( \Psi_c^\dagger \nabla \Psi_c - (\nabla \Psi_c^\dagger) \Psi_c \right),$$

with  $\Psi_c$  the component of the wave function of state  $c$ .

We have for the inelastic channels

$$\frac{1}{V} \oint_S \vec{j}_c \cdot d\vec{S} = \sigma_c \quad c \neq c_0, \quad \text{so that} \quad \sigma_r = \sigma_{abs} + \sum_{c \neq c_0} \sigma_c.$$

That is, the elastic absorption cross section is the sum of the total absorption cross section and the inelastic excitation cross sections.

## Cross sections and transmission coefficients

Using the asymptotic form of the wave function, the elastic absorption cross section may be calculated,

$$\sigma_r = \frac{1}{(2s+1)(2I_0+1)} \frac{\pi}{k_{c_0}^2} \sum_{\substack{l' \\ l \\ ij}} (2J+1) \left( \delta_{l'l} \delta_{j'j} - \left| S_{l'j'c_0, ljc_0}^J \right|^2 \right).$$

It is a sum of the contributions of the elastic S-matrix elements.

The total absorption cross section may be reduced to a similar form,

$$\sigma_{abs} = \frac{1}{(2s+1)(2I_0+1)} \frac{\pi}{k_{c_0}^2} \sum_{\substack{l' \\ l \\ ij}} (2J+1) T_{ljc_0, ljc_0}^J,$$

where we have introduced the coupled-channel transmission coefficients, which in matrix form are

$$T_j = 1_j - S_j^\dagger S_j.$$

For neutrons, we may define the total cross section as the sum of the elastic and the elastic absorption ones,

$$\sigma_{tot} = \sigma_{el} + \sigma_r = \frac{1}{(2I_0+1)} \frac{\pi}{k_{c_0}^2} \sum_{\substack{l' \\ l \\ ij}} (2J+1) (1 - \text{Re } S_{ljc_0, ljc_0}^J).$$

The total cross section measures the flux lost from the incident plane wave. It takes into account scattering of any type.

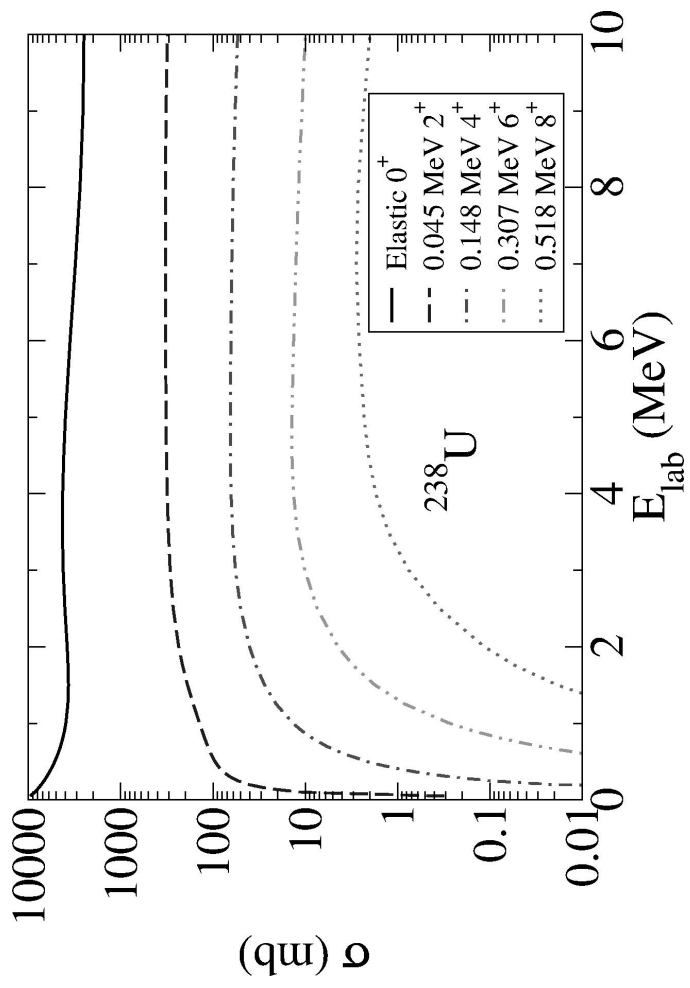
## An example – Rotational excitation of $^{238}\text{U}$

Let us consider excitation of the ground state rotational band of  $^{238}\text{U}$  through the  $8^+$  state. For  $J=1/2$ ,  $1+2+2+2+2=9$  coupled channels are involved. For large values of the total angular momentum, we have  $1+5+9+13+17=45$  coupled channels in each partial wave.

The cross sections of the first excited states increase rapidly above their thresholds. The cross sections of the more highly excited states increase more smoothly.

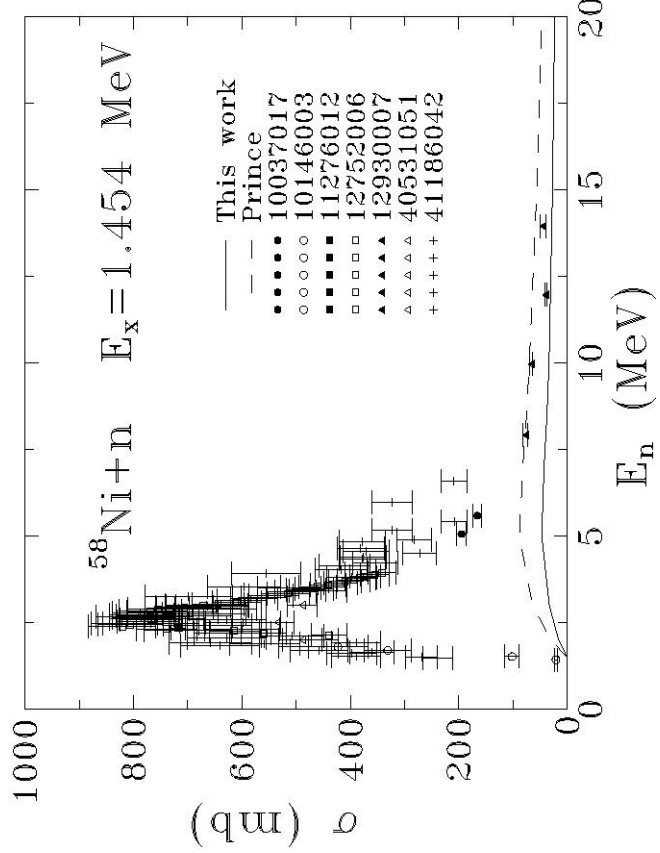
All of the cross sections decrease very slowly at high energy.

The high energy values of the cross sections decrease by a factor of about 5 for each state as one ascends the rotational band in excitation energy.



## Comparison with experiment

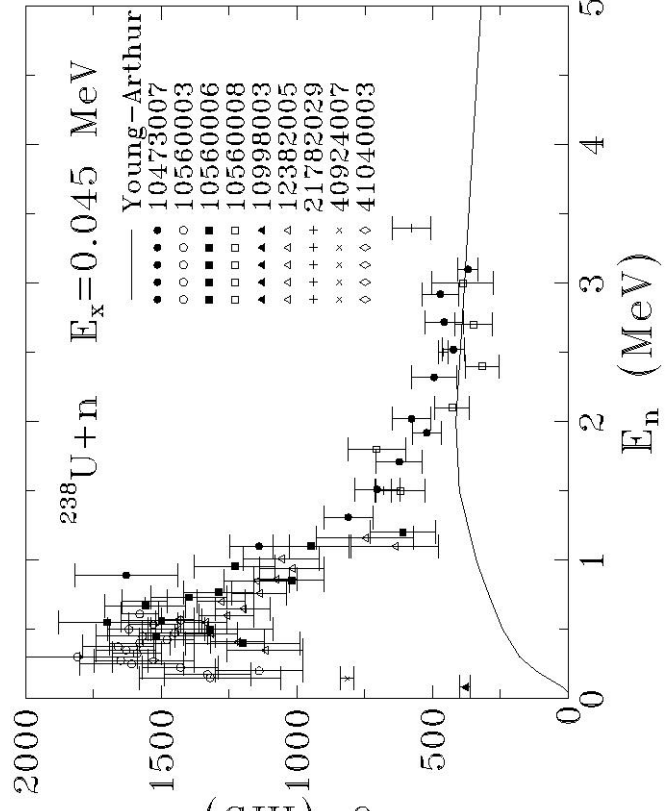
Inelastic cross sections are dominated by the contribution from the compound nucleus at low energies, as seen here for the first excited states of  $^{58}\text{Ni}$  and  $^{238}\text{U}$ .



The two calculations of the  $^{58}\text{Ni}$  inelastic cross section use the same

value of  $\beta_2=0.2$ , yet yield cross sections that differ by almost a factor of two due to differences in the optical potentials.

The cross section for excitation of the rotational state in  $^{238}\text{U}$  is 5 to 10 times greater than that of the vibrational state in  $^{58}\text{Ni}$ , mainly due to the factor of 30 difference in their excitation energies.



# The Lippmann-Schwinger equation -- I

The integral representation of the wave equation, the Lippmann-Schwinger equation,

$$\Psi = \Psi_0 + (E^+ - H_0)^{-1} U' \Psi = \Psi_0 + G_0^+ U' \Psi, \quad \text{where } (E - H_0) \Psi_0 = 0,$$

is often very useful for the analysis and solution of scattering problems.

Here,  $G_0^+$  is the outgoing-wave Green's function and  $\Psi_0$  a wave function with an incoming wave boundary condition. It is usually most convenient to place the single-channel optical potential in the  $H_0$  of the equation and only the couplings between states in  $U'$ .

For the single-channel optical model, we can define incoming/outgoing-wave solutions,  $h_{lc}^{j\pm}(r)$ , of the wave equation,

$$\left( \frac{d^2}{dr^2} - \frac{l(l+1)}{r^2} + k_c^2 - \frac{2\mu}{\hbar^2} (U_{cen,c}(r) + d_l^j U_{so,c}(r)) \right) h_{lc}^{j\pm}(r) = 0,$$

where the spin-orbit factor is  $d_l^j = d_{so}(j(j+1) - l(l+1) - s(s+1))/2$ .

Asymptotically, these solutions behave as incoming/outgoing Coulomb (free) waves,

$$h_{lc}^{j\pm}(r) \rightarrow H_{lc}^{j\pm}(r) = e^{\mp i\sigma_{lc}} (G_{lc}(r) \pm iF_{lc}(r)).$$

## The Lippmann-Schwinger equation -- II

The solution to the single-channel Schrödinger equation that is regular at the origin is given in terms of the incoming/outgoing solutions and the S-matrix as

$$\psi_{lc}^{j+}(r) = \frac{i}{2} \left( h_{lc}^{j-}(r) - h_{lc}^{j+}(r) e^{2i\sigma_{lc}} S_{0lc}^j \right) = \psi_{lc}^j(r) e^{i\sigma_{lc}},$$

which is just the single-channel wave function of the partial wave expansion. We have merely relabeled the S-matrix as  $S_0$ .

The single-channel Green's function may be decomposed in partial waves as

$$G_{0c}^+(\vec{r}, \vec{r}') = \frac{1}{rr'} \sum_{ljn} \mathfrak{D}_{ls}^{jn}(\hat{r}) g_{lc}^{j+}(r, r') \mathfrak{D}_{ls}^{jn\dagger}(\hat{r}'),$$

where

$$g_{lc}^{j+}(r, r') = -\frac{2\mu}{\hbar^2 k_c} \psi_{lc}^j(r_\angle) e^{i\sigma_{lc}} h_{lc}^{j+}(r_\angle).$$

The complete single-channel Green's function for the coupled-channels problem may then composed as

$$G_0^+(\vec{r}, \vec{r}') = \sum_{cN_c} |cI_c N_c\rangle G_{0c}^+(\vec{r}, \vec{r}') \langle cI_c N_c|$$

$$= \frac{1}{rr'} \sum_{ljn} \mathfrak{D}_{lsj}^{JM}(\hat{r}) g_{lc}^{j+}(r, r') \mathfrak{D}_{lsj}^{JM\dagger}(\hat{r}).$$

# The Lippmann-Schwinger equation -- III

In terms of the channel matrices, the Green's function  $G_0^+$  takes the form

$$G_0^+(\vec{r}, \vec{r}') = \frac{1}{rr'} \sum_{JM} \langle \hat{r} | JM \rangle G_{0J}^+(r, r') \langle JM | \hat{r}' \rangle,$$

where we have grouped the appropriate Green's functions in diagonal matrices,

$$g_{lc}^{j+}(r, r') \delta_{l'l} \delta_{j'j} \delta_{c'c} \rightarrow G_{0J}^+(r, r').$$

In terms of these, we can write the contribution to the Lippmann-Schwinger equation of each partial wave as

$$\Psi_J(r) = \Psi_{0J}(r) + \int_0^\infty dr' G_{0J}^+(r, r') U'_J(r') \Psi_J(r').$$

Substituting the large- $r$  expressions for the wave functions,

$$\Psi_{0J}^+ \rightarrow \frac{i}{2} \left( H_J^-(r) - H_J^+(r) e^{i\sigma_J} \bar{S}_{0J} e^{i\sigma_J} \right) e^{-i\sigma_J},$$

and using flux conservation to normalize the S-matrix,  $S_J = K_J^{1/2} \bar{S}_J K_J^{-1/2}$ , we obtain

$$S_J = S_{0J} + 2i \frac{2\mu}{\hbar^2} K_J^{-1/2} \int_0^\infty dr' \Psi_{0J}(r') U'_J(r') \Psi_J(r') K_J^{-1/2}.$$

# The distorted-wave Born approximation (DWBA)

The Lippmann-Schwinger equation,

$$\Psi_J(r) = \Psi_{0J}(r) + \int_0^\infty dr' G_{0J}^+(r, r') U'_J(r') \Psi_J(r'),$$

here in partial wave form, contains the wave function  $\Psi_J(r)$  on both the right and left sides of the equation. This can be used to advantage when the coupling potential  $U'$  is small. We then expect the wave function  $\Psi_J$  to be little different from the uncoupled one  $\Psi_{0J}$ , so that we have, to first order,

$$\Psi_J^{(1)}(r) = \Psi_{0J}(r) + \int_0^\infty dr' G_{0J}^+(r, r') U'_J(r') \Psi_{0J}(r').$$

The corresponding DWBA S-matrix is

$$S_J^{(1)} = S_{0J} + 2i \frac{2\mu}{\hbar^2} K_J^{-1/2} \int_0^\infty dr' \Psi_{0J}(r') U'_J(r') \Psi_{0J}(r') K_J^{-1/2}.$$

The DWBA approximation may be extended to higher orders by substituting the solution of the previous order in the Lippmann-Schwinger equation. The second-order solution, for example, is obtained by substituting the first order solution in the integral equation. However, the DWBA is usually not used above the second-order.

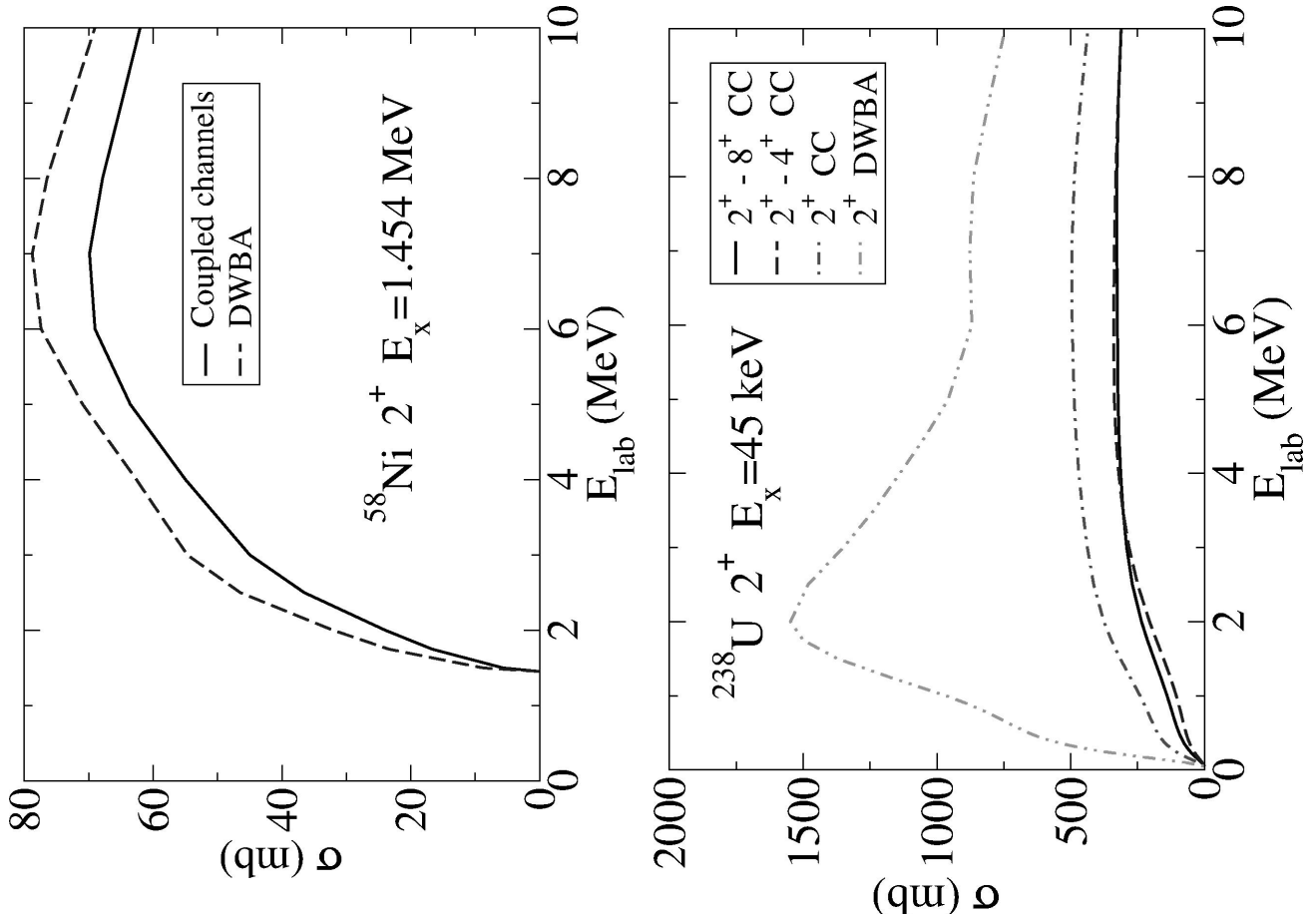
## Limit of the DWBA

Two examples give us an idea of when the DWBA might be applied to inelastic scattering.

The DWBA provides a reasonable approximation to excitation of a vibrational state such as the  $2^+$  one in  $^{58}\text{Ni}$ . However, it greatly overestimates the excitation of a strongly-excited rotational state, such as the  $2^+$  one in  $^{238}\text{U}$ .

In general, the DWBA overestimates the inelastic cross section, since it does not take into account transitions back to the ground state.

In the case of  $^{238}\text{U}$ , we note that transitions to other states of the rotational band can also be important.



## The ECIS method -- I

The ECIS method (Equations Couplées en Itérations Séquentielles) is an alternative to the standard coupled-channels method. It is based on the Lippmann-Schwinger equation,

$$\Psi_j(r) = \Psi_{0j}(r) + \int_0^\infty dr' G_{0j}^+(r, r') U'_j(r') \Psi_j(r'),$$

given here in partial wave form. The ECIS method uses a decomposition of the optical potential into the single-channel potentials, placed in  $H_0$ , and the couplings between states, which are put in  $U'$ . It assumes that the states are arranged in order of decreasing coupling with the ground state.

Beginning with the ground-state (state 0) single-channel wave function, the ECIS method:

- Calculates the wave function of the first excited state (state 1) using that of state 0,  
 $\vdots$
- Calculates the wave function of the second excited state (state 2) using those of states 0 and 1,
- Calculates the wave function of the ground state (state 0) using those of states 1 through  $n$ .

## The ECIS method -- II

The calculation of the wave functions for each of the states is then repeated in the same order, using for the other states the last wave function that was calculated, either from the same iteration or from the preceding one.

The set of calculations, beginning with the first excited state through the ground state, are iterated until convergence is achieved.

The method is extremely efficient in cases in which the coupling is small, such as that of the  $2^+$  vibrational state in  $^{58}\text{Ni}$ . The standard coupled channels method must solve a matrix equation, which requires a processing time similar to that of performing an ECIS iteration for each of the coupled channels. In weakly-coupled problems, convergence may occur in a few iterations, making the method the more efficient of the two.

In strongly coupled problems, such as that of the ground state rotattonal band in  $^{238}\text{U}$ , the opposite is the case. The convergence of ECIS iterations can be much slower than solution using the standard method, when convergence occurs at all.

# Single-channel calculations with ECIS95

To perform a single-channel optical model calculation, we have to furnish information on:

- The system –  $Z_p$ ,  $A_p$ ,  $Z_t$ ,  $A_t$ , and  $E_{cm} = A_p E_{lab} / (A_p + A_t)$ ,  $I^\pi$  of target;
- The optical potential parameters –  $V$ ,  $V_s$ ,  $W$ ,  $W_s$ ,  $V_{so}$  and  $W_{so}$  and the geometrical parameters – the reduced radii  $r_i$  and diffusivities  $a_i$ ;
- Quantities to be calculated – cross sections (automatic), S-matrix elements (in the form  $C = (S-1)/2i$ ), transmission coefficients, angular distributions and/or polarizations printed and/or plotted.

ECIS95 -- by J. Raynal -- does not calculate several basic low-energy observables -- strength functions and the scattering radius.

ECIS95 can fit parameters to experimental data – integrated and differential cross sections, polarizations, and others, by minimizing

$$\chi^2 = \sum_i \left[ (\sigma_i^{cal} - \sigma_i^x) / \Delta \sigma_i^x \right]^2.$$

ECIS95 cannot use or adjust energy-dependent parameters.

PRECIS – a utility code to facilitate input preparation.

## Exercise 1 – n + $^{58}\text{Ni}_{28}$

Spherical Optical Model Calculation: Using the program PRECIS, generate an input data file for the ECIS95 code for neutrons incident on  $^{58}\text{Ni}_{28}$  at 0.1, 1.0 and 10.0 MeV in the laboratory system that:

- Includes only the  $0^+$   $^{58}\text{Ni}$  ground state,
- Uses the global optical potential parameters of Wilmore-Hodgson,
- Prints the C-matrix elements,  $C=(S-1)/2i$ , and
- Calculates and plots the differential elastic cross section in  $10^\circ$  intervals from  $0^\circ$  to  $180^\circ$ .

Look at the contents of the input data file and try to identify the parameters that you entered.

In the output file, for each value of the incident energy,

- Find the optical potential parameters,
- Find the C-matrix elements, and
- Find the integral and differential cross sections.

Are the optical potential parameters constant?

# A dialogue with the code PRECIS – Exercise 1 – 1

To prepare an input file for ECIS95, begin by entering the name of your file.

ecis-ex1

Enter the title that you wish to appear on the output.

n+58Ni -- Spherical optical model -- Wilmore-Hodgson parameters

Enter 1 if the logical switches are to be printed  
0 otherwise.

1

Enter the number corresponding to the projectile.

- 1 - neutron
- 2 - proton
- 3 - deuteron
- 4 - tritium
- 5 - helium-3
- 6 - alpha

1

Enter the charge, mass, spin and parity (+1 or -1) of the target.

28. 58. 0. 1.

# A dialogue with the code PRECIS – Exercise 1 -- 2

Enter 1 to use a global potential,

0 to enter the potential parameters.

1

Enter the number corresponding to the potential to be used.

- 1 - Wilmore-Hodgson ( 40 < A E < 10 )
- 2 - Bechetti-Greenless ( 40 < A 10 < E < 50 )
- 3 - Ferrer-Rapaport ( 24 < A < 209 E = 11 )
- 4 - Cindro-Bersillon
- 5 - MacLland-Young ( actinides )

1

For each of the potentials vc, w, vso and wso, enter 1 if its deformation is to be taken into account, otherwise enter 0.

0 0 0

Enter the number of excited states to be used.

0

# A dialogue with the code PRECIS – Exercise 1 -- 3

Enter 1 to include the contribution of the compound nucleus,  
0 otherwise.

0

Enter 1 to use the standard coupled channels method,  
0 to use the ECIS method.

1

Enter 1 if the C-matrix elements,  $C=(S-1)/2i$ , are to be printed  
0 otherwise.

1

Enter 1 if the transmission coefficients are to be written on unit7,  
0 otherwise.

1

Enter 1 if angular distributions are to be calculated,  
0 otherwise.

1

Enter the first angle, the stepsize and the last angle to be used  
to calculate the angular distributions. (Angles in degrees.)  
0 . 10 . 180 .

Enter 1 if angular distributions are to be plotted,  
0 otherwise.

0

# A dialogue with the code PRECIS – Exercise 1 -- 4

Enter 1 if experimental data are to be input,  
0 otherwise.

0

Enter the number of projectile energies at which calculations will  
be performed.

3

Enter 1 if the projectile energies are to be equally spaced,  
0 otherwise.

0

Enter the energies (in MeV in the lab frame).

0 .1 . 10 .

Enter 1 to prepare the input data to another ECIS95 calculation,  
0 to stop.

0

Your input to ECIS95 is in file ecis-ex1.in.

---

To run the code ECIS95 with this input file, type:

```
ecis95 <ecis-ex1.in >ecis-ex1.out
```

The results of the run will be written to the file ecis-ex1.out. The transmission  
coefficients will be printed in a separate file on unit 7.

# Exercise 1 – ECIS95 input

n+58Ni -- Spherical optical model – Wilmore-Hodgson parameters  
FFFFFTFFFFFFTFFTFTFFFFFTFFFFTTTTTFFFTFFTTTFFFTFFF  
0 1 0 0  
0. 000000 0. 000000 0. 000000 0. 000001 0. 000001 0. 000001  
0. 00 0 1+ 0. 100000 0. 500000 1. 00866 58. 00000 0. 00000  
0  
46. 98329 1. 28982 0. 66000  
0. 00000 1. 00000 0. 60000  
0. 00000 1. 25049 0. 48000  
9. 51470 1. 25049 0. 48000  
7. 00000 1. 28982 0. 66000  
0. 00000 1. 28982 0. 66000  
1. 25000 0. 00000 0. 00000  
0. 00000 1. 25000 0. 00000  
0. 00000 10. 00000 180. 00000  
T 14 0 0 1 2 4 5 7 8 10 11 12 13 14 16 17  
1. 00000 46. 74182 1. 28982 0. 00000 1. 00000 0. 00000 0. 00000 1. 25049  
9. 46700 1. 25049 0. 48000 7. 00000 1. 28982 0. 00000 0. 00000 1. 28982  
F 14 0 2 4 5 7 8 10 11 12 13 14 16 17  
10. 00000 44. 22200 1. 28982 0. 00000 1. 00000 0. 00000 0. 00000 1. 25049  
8. 99000 1. 25049 0. 48000 7. 00000 1. 28982 0. 00000 0. 00000 1. 28982  
FIN

## Coupled-channels calculations with ECIS95

To perform a coupled-channels optical model calculation, we have to furnish the same information as before on:

- The system –  $Z_p, A_p, Z_t, A_t$ , and  $E_{cm} = A_t E_{lab} / (A_p + A_t)$ ,  $I^\pi$  of target +  $I^\pi, E_x$  and structure (phonon number) of excited states;
- The optical potential parameters –  $V, V_s, W, W_s, V_{so}$  and  $W_{so}$  and the geometrical parameters – the reduced radii  $r_i$  and diffusivities  $a_i$  + excitation model (vib/rot),  $\beta_i$  and expansion parameters;
- Quantities to be calculated – cross sections (automatic), S-matrix elements (in the form  $C = (S-1)/2i$ ), transmission coefficients, angular distributions and/or polarizations printed and/or plotted.

ECIS95 -- by J. Raynal -- can fit parameters to experimental data – integrated and differential elastic and inelastic cross sections, polarizations, and others.

ECIS95 can perform standard and ECIS coupled-channels calculations.

Transmission coefficients require that the entire S-matrix be calculated, which is usually more efficient using the standard method. The ECIS method permits the inclusion of a deformed spin-orbit interaction.

DWBA calculations may be performed by restricting the ECIS method to one or two iterations and restricting the interaction appropriately.

## Exercise 4 – n + $^{58}\text{Ni}_{28}$

Deformed Optical Model Calculation: Using the program PRECIS, generate an input data file for the ECIS95 code for neutrons incident on  $^{58}\text{Ni}_{28}$  that:

- Includes the  $0^+$   $^{58}\text{Ni}$  ground state and the  $2^+$  excited state at 1.454 MeV as a vibrational state,

- Uses the following optical potential parameters:

--  $r_V=1.27$  fm,  $a_V=0.75$  fm,  $V_0=48.87$  MeV,  $V_1=-0.369$  and  $V_2=0.002$  MeV $^{-1}$ ,  
--  $r_{Ws}=1.34$  fm,  $a_{Ws}=0.375$  fm,  $W_{s0}=14.3$  MeV,  $W_{s1}=0.16$  and  $W_{s2}=-0.006$  MeV $^{-1}$ ,  
--  $r_{Vs0}=1.27$  fm,  $a_{Vs0}=0.75$  fm,  $V_{so0}=6.75$  MeV,

with a phonon amplitude  $\beta_2=0.2$  and all other potential strengths zero,

- Uses the standard coupled-channels method,
- Includes the file of experimental data ecis-ex4.dat, and
- Adjusts the phonon amplitude  $\beta_2$ .

Look at the contents of the input data file and try to identify the parameters that you entered.

In the output file,

- Find the final value of the adjusted parameter.
- Find the comparisons between the experimental data and the calculations.

# A dialogue with the code PRECIS – Exercise 4 -- 1

To prepare an input file for ECIS95, begin by entering the name of your file.

ecis-ex4

Enter the title that you wish to appear on the output.

n + 58Ni -- Optical parameters fit to data set

Enter 1 if the logical switches are to be printed  
0 otherwise.

1

Enter the number corresponding to the projectile.

1 - neutron

2 - proton

3 - deuteron

4 - tritium

5 - helium-3

6 - alpha

1

Enter the charge, mass, spin and parity (+1 or -1) of the target.

28. 58. 0. 1

# A dialogue with the code PRECIS – Exercise 4 -- 2

Enter 1 to use a global potential,

0 to enter the potential parameters.

0

Enter 1 if dispersion terms are to be taken into account,  
0 otherwise.

0

Enter r0(v), r1(v), av, v0, v1, v2, v1 and cv,

where  $v = v0 + v1 * e + v2 * e^{**} 2 + v1 * \ln(e) + cv * \sqrt{e}$  and  
 $r0 = r0(v) + r1(v) * e$ .

1.27 0. 0.75 48.87 -0.369 0.002 0. 0.

Enter r0(ws), r1(ws), aws, ws0, ws1, ws2, ws1 and cws,  
where  $ws = ws0 + ws1 * e + ws2 * e^{**} 2 + ws1 * \ln(e) + cws * \sqrt{e}$   
and  $rws0 = r0(ws) + r1(ws) * e$ .

1.34 0. 0.375 14.13 0.16 -0.006 0. 0.

# A dialogue with the code PRECIS – Exercise 4 -- 3

Enter  $r0(w)$ ,  $r1(w)$ ,  $aw$ ,  $w0$ ,  $w1$ ,  $w2$ ,  $wl$  and  $cw$ ,

where  $w = w0 + w1 * e + w2 * e^{**} 2 + wl * \ln(e) + cw * \sqrt{e}$  and  
 $rw0=r0(w) + r1(w) * e$ .

1.2 0. 0.6 0. 0. 0. 0.

Enter  $r0(vso)$ ,  $r1(vso)$ ,  $avso$ ,  $vso0$ ,  $vsol$ ,  $vso2$ ,  $vsol$  and  $cuso$ ,  
where  $vso=vso0 + vsol * e + vso2 * e^{**} 2 + vsol * \ln(e) + cuso * \sqrt{e}$   
and  $rvso0=r0(vso) + r1(vso) * e$ .

1.267 0. 0.75 6.75 0. 0. 0.

Enter  $rc0$  and  $ewmax$ .

1.25 12.

For each of the potentials  $vc$ ,  $w$ ,  $vso$  and  $wso$ , enter 1 if its  
deformation is to be taken into account, otherwise enter 0.

0 0 0 0

# A dialogue with the code PRECIS – Exercise 4 -- 4

Enter the number of excited states to be used.

1

Enter 0 to use the vibrational model,  
1 to use the rotational model.

0

Enter the number of distinct phonons to be used.

1

For each phonon, enter its angular momentum and its amplitude.

2 0 . 2

Enter the energy (in MeV), spin and parity (+1 ou -1) of the first excited state.

1.454 2 . 1.

Enter the number of phonons used to describe the first excited state.

1

Enter the number(s) identifying the phonon(s) used to describe this state  
phonon no.

1 2

1

# A dialogue with the code PRECIS – Exercise 4 -- 5

Enter 1 to include the contribution of the compound nucleus,  
0 otherwise.

0

Enter 1 to use the standard coupled channels method,  
0 to use the ECIS method.

1

Enter 1 if the C-matrix elements,  $C=(S-1)/2i$ , are to be printed  
0 otherwise.

1

Enter 1 if the transmission coefficients are to be written on unit 7,  
0 otherwise.

1

Enter 1 if angular distributions are to be calculated,  
0 otherwise.

0

Enter 1 if experimental data are to be input,  
0 otherwise.

1

# A dialogue with the code PRECIS – Exercise 4 -- 6

Enter 1 if experimental angular distributions are to be plotted,  
0 otherwise.

0

Enter 1 if parameters are to be adjusted,  
0 otherwise.

1

For each of the following parameters, enter the precision desired of  
the fit.

If the precision is given as 0., the parameter will not be adjusted.

v, rv0, av

0. 0. 0.

vs, rvs0, avs

0. 0. 0.

ws, rws0, aws

0. 0. 0.

w, rw0, aw

0. 0. 0.

vso, rvso0, avso

0. 0. 0.

# A dialogue with the code PRECIS – Exercise 4 -- 7

wso, rwso0, awso

0. 0. 0.

The amplitude of the multipolarity 2 phonon

0.01

Enter the number of projectile energies at which calculations will be performed.

7

Enter 1 if the experimental data are on file,  
0 if they will be input.

1

Enter the complete name of the data file.

ecis-ex4.dat

Enter 1 to prepare the input data to another ECIS95 calculation,  
0 to stop.

0

Your input to ECIS95 is in file ecis-ex4.in.

# The possibilities of ECIS95

The aim of these lectures has been to provide an introduction to the basic problems in nuclear physics to which ECIS95 may be applied. For lack of time, we have discussed only the simplest applications. ECIS95 is capable of many other types of calculations. Among these are:

- The use of more elaborate macroscopic models, such as the anharmonic vibrator, the asymmetric rotor or the vibrational-rotational model,
- Inclusion of the compound nucleus contribution to cross sections, in a single-channel model or the Engelbrecht-Weidenmüller coupled-channel one,
- Dirac optical model calculations,
- Heavy-ion optical model calculations,
- Long-range Coulomb excitation,
- Projectile and target excitation,
- Transfer reactions within a zero-range DWBA.

It can be a powerful tool in the hands of those who know how to use it.